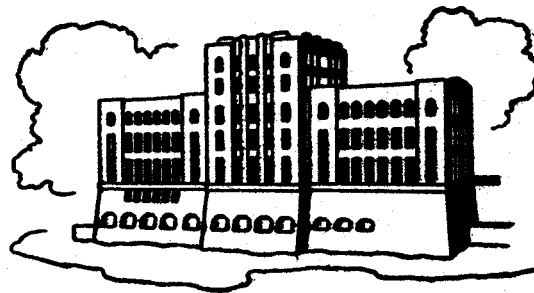


# ON THE DISTRIBUTION AND DEVELOPMENT OF MEAN-FLOW AND TURBULENCE CHARACTERISTICS IN JET AND WAKE FLOWS

by

Eduard Naudascher

Sponsored by  
Fluid Dynamics Branch  
Office of Naval Research  
U.S. Navy Department  
Contract Nonr 1611(03)



IIHR Report No. 110

Iowa Institute of Hydraulic Research  
The University of Iowa  
Iowa City, Iowa

August 1968

This document has been approved for public  
release and sale; its distribution is unlimited.

ON THE DISTRIBUTION AND  
DEVELOPMENT OF MEAN-FLOW AND  
TURBULENCE CHARACTERISTICS  
IN JET AND WAKE FLOWS

by

Eduard Naudascher

Sponsored by  
Fluid Dynamics Branch  
Office of Naval Research  
U.S. Navy Department  
Contract Nonr 1611(03)

IIHR Report No. 110

Iowa Institute of Hydraulic Research  
The University of Iowa  
Iowa City, Iowa

August 1968

This document has been approved for public  
release and sale; its distribution is unlimited.

## ABSTRACT

The lateral distributions of various mean-flow and turbulence characteristics, as obtained from measurements in axisymmetric jets and wakes, are shown to conform to a new concept of self-preservation. The development downstream from the flow origin of representative cross-sectional values of the turbulence shear stress  $\overline{\rho u'v'}$ , turbulence normal stress  $\overline{\rho u'^2}$ , and the maximum mean-velocity difference  $U_d$ , as well as the development of some nondimensional ratios thereof, is presented for the following free-turbulence flows: plane free jets and wall jets with ambient streams, axisymmetric jets in coaxial streams with different ratios of jet to free-stream velocity, and wakes behind a slender spheroid, a disk, a square plate, and a self-propelled body of revolution. The results indicate that in the case of axisymmetric free-shear flows, similarity according to the conventional definition is not even approached asymptotically and that the conditions of flow generation have a greater influence on the downstream flow development than has been assumed previously.

On the Distribution and Development of Mean-Flow and  
Turbulence Characteristics in Jet and Wake Flows

INTRODUCTION

In the further pursuit of a general similarity analysis for the prediction of mean-flow and turbulence characteristics of any axially or plane symmetric free-turbulence flow, it became evident that a re-evaluation of experimental data was needed in order to provide material for checking the validity of the hypotheses on the turbulence structure. Because of conflicting results for seemingly related flows, this endeavor turned out to be more laborious than anticipated. It finally involved reduction on a common basis of mean-flow and turbulence measurements in plane free jets and wall jets with ambient streams, axisymmetric jets in coaxial streams for a variety of ratios of jet to free-stream velocity, wakes behind slender and blunt axisymmetric bodies, and the wake of an axisymmetric self-propelled body. Rather than using the outcome of this study merely as a justification for the new similarity analysis, the results are presented here in their own right for the conclusions they permit concerning the interdependence of mean-flow and turbulence characteristics.

Part of the general similarity analysis, which served as the basis for the data re-evaluation, has been described earlier (Naudascher 1967). A complete presentation of this analysis will be submitted to a technical journal in the near future.

ANALYTICAL CONSIDERATIONS

According to a new similarity concept, presented in a preceding report (Naudascher 1967), self-preservation is defined as follows:

$$\frac{\bar{u}_d^2 + U\bar{u}_d}{U^{*2} + UU^*} = f(\eta) \quad (1)$$

$$\frac{\bar{q}^2}{q^{*2}} = h(\eta) \quad , \quad \frac{\overline{u'^2}}{q^{*2}} = h_1(\eta) \quad , \quad \frac{\overline{v'^2}}{q^{*2}} = h_2(\eta) \quad (2)$$

$$\frac{\bar{e}}{\tau^*} = k(\eta) \quad (3)$$

wherein  $\eta \equiv y/\ell$ , and  $\ell$ ,  $U^*$ ,  $q^{*2}$ , and  $\tau^{*2}$  represent a length scale and

dynamic scales, respectively (i.e., characteristic values of the width of the diffusion zone, of the mean-velocity difference  $\bar{u}_d$ , of  $\bar{q}^2 = \overline{u'^2} + \overline{v'^2} + \overline{w'^2}$ , and of  $\bar{\tau} = -\overline{\rho u'v'}$ ). The essential distinction from the conventional definitions

$$\frac{\bar{u}_d}{U^*} = g(\eta) \quad (4a)$$

$$\frac{\bar{\tau}/\rho}{U^{*2}} = g_1(\eta) \quad (4b)$$

$$\frac{\bar{q}^2}{U^{*2}} = g_2(\eta) \quad (4c)$$

consists of, first, the abandonment of a priori assumptions regarding the inter-relationship between mean-flow and turbulence characteristics (as Eqs. 4b and c entail), and, second, the selection of a momentum parameter (Eq. 1) which makes the self-preservation function comply with the restrictions imposed by the equations of motion without the necessity of limiting the applicability of the results through simplifications as severely as before. In the preceding report, it was also pointed out that compatibility with the equations of motion would require replacement of Eq. 3 by

$$\frac{(\bar{\tau}/\rho)\partial\bar{u}/\partial y}{P^*} = K(\eta) \quad (5)$$

that is, by a self-preserving expression for a turbulence-production parameter rather than for the turbulence shear stress. (The denominator in this expression stands for a value of the numerator that is characteristic for a cross-section, as will be defined later.) However, because the parameter of Eq. 3 is of greater practical use, the consequences of the assumption contained in Eq. 5 was not pursued further at that time.

In the following, let it be assumed, that there exists self-preservation as defined by Eqs. 1, 2, and 5, and that the dissipation length  $\lambda$ , defined by  $\overline{(\partial u'/\partial x)^2} \equiv \overline{u'^2}/\lambda^2$ , is independent\* of  $y$ . Substitution of Eqs. 1, 2a, 4a, and 5 into the turbulence-energy equation (Naudascher 1967, Eq. 22) yields then

$$\frac{U+U^*}{l} \left[ l \frac{dq^{*2}}{dx} I_3 - q^{*2} \frac{dl}{dx} I_4 \right] + \rho^* I_5 + \nu \frac{q^{*2}}{\lambda^2} I_6 = 0 \quad (6)$$

\*Actually, a self-preserving variation  $\lambda = \lambda(\eta)$  would lead to essentially the same result.

with

$$I_3 \equiv \frac{1}{2} \int_0^{\eta_0} \frac{f}{g} h \eta^j d\eta, \quad I_4 \equiv \frac{1}{2} \int_0^{\eta_0} \frac{f}{g} \frac{dh}{d\eta} \eta^{j+1} d\eta, \quad I_5 \equiv \int_0^{\eta_0} K \eta^j d\eta, \quad I_6 \equiv 5 \int_0^{\eta_0} h \eta^j d\eta \quad (7)$$

in which  $\eta_0 = y_0/l > b/l$  (see Fig. 1),  $j = 0$  for plane symmetry and  $j = 1$  for axial symmetry. While  $I_3$  and  $I_4$  will vary slightly with  $x$ , except for regions for which the functions  $f$  and  $g$  are both self-preserving (i.e., for  $U/U^* \ll 1$  or  $U^*/U \gg 1$ ),  $I_5$  and  $I_6$  are numerical constants, in accordance with Eqs. 2 and 5. In shear flows in which the cumulative convection rate of turbulence kinetic energy has a negligible rate of change as compared to the rates of change of the cumulative production and dissipation rates, the first term of Eq. 6 can be ignored (for verification, see Rouse 1960, Sami, Carmody and Rouse 1967, and Chevray 1967), and Eq. 6 yields

$$\frac{q^{*2} \nu}{P^* \lambda^2} = - \frac{I_5}{I_6} \approx \text{const} \quad (8)$$

Additional information regarding the functions  $U^*(x)$  and  $l(x)$  can be gained from the integrated form of the momentum equation (Naudascher 1967, Eq. 13 or 18). For shear flow generated by an external force, be it the drag of a towed body or the thrust of a propeller or a jet, the term containing the turbulence stresses in the momentum equation can be considered as small compared to the mean-velocity term and hence can be neglected. This simplification (which is verified, for example, by the measurements in the wake of a cylinder by Townsend 1948, 49, 56) lead to the condition

$$(U^{*2} + UU^*) l^{j+1} = H/I_1 = \text{const} \quad (9)$$

with

$$I_1 \equiv \int_0^{\eta_0} f \eta^j d\eta \quad (10)$$

which is valid for unconfined shear flows and, provided the effect of boundary layer growth is negligible, also for shear flows confined by parallel walls (for the definition of  $H$ , see Eq. 23 or Naudascher 1967, p. 6 and 7). For these cases, therefore, the momentum equation does not require further simplifications or restrictions as long as the special form of self-preservation expressed by Eq. 1 is adopted.

A further condition for self-preservation is obtained from the mean-energy equation (Naudascher 1965, Eq. 19). After substitution of Eqs. 1, 2, 4a, and 5 into this equation along with Eq. 9 one obtains

$$H \frac{d}{dx} \left[ U + U^* \frac{I_7}{I_1} \right] + \rho^* l^{j+1} I_5 + (U^* + U) l^j \left[ l \frac{dq^{*2}}{dx} I_3' - q^{*2} \frac{dl}{dx} I_4' \right] = 0 \quad (11)$$

with

$$I_7 \equiv \frac{1}{2} \int_0^{\eta_0} f g \eta^j d\eta, \quad I_3' \equiv \int_0^{\eta_0} \frac{f}{g} (h_1 - h_2) \eta^j d\eta, \quad \text{and} \quad I_4' \equiv \int_0^{\eta_0} \frac{f}{g} \frac{\partial(h_1 - h_2)}{\partial \eta} \eta^{j+1} d\eta \quad (12)$$

Like Eqs. 6 and 9, Eq. 11 applies to both unconfined flow and flow confined by parallel walls with negligible boundary-layer growth.

For a region of flow in which the convection rate of turbulence energy and hence the last term of Eq. 11 is negligible, Eq. 11 leads to

$$\rho^* l^{j+1} = - \frac{H}{I_5} \frac{d}{dx} \left[ U + U^* \frac{I_7}{I_1} \right] \quad (13)$$

Three conditions, Eqs. 8, 9, and 13, have thus been derived for a determination of the five unknown functions  $U^*(x)$ ,  $q^*(x)$ ,  $l(x)$ , and  $\lambda(x)$ . Although two more conditions are still needed, an important conclusion can already be drawn with respect to the interrelationship between mean-flow and turbulence characteristics. When  $P^*$  and a characteristic shear stress  $\tau^*$  are defined as

$$P^* \equiv \int_0^{\infty} (-\overline{u'v'}) \frac{\partial \bar{u}_d}{\partial y} (2\eta)^j d\eta \quad (14)$$

and

$$\frac{\tau^*}{\rho} \equiv \overline{u'v'}^* \equiv - \int_0^{\infty} \overline{u'v'} (2\eta)^j d\eta \quad (15)$$

we can express this interrelationship by first modifying Eq. 15 through Eqs. 1 and 5 to

$$\frac{u'v'^*}{U^{*2}} = \frac{P^* l}{U^{*3}} \int_0^{\infty} \frac{2\bar{u}_d + U}{U^* + U} \frac{k}{df/d\eta} (2\eta)^j d\eta = I_9 \frac{(2I_8/I_9)U^* + U}{U^* + U} \frac{P^* l}{U^{*3}} \quad (16)$$

with

$$I_8 \equiv \int_0^{\infty} g \frac{K}{df/d\eta} (2\eta)^j d\eta \quad \text{and} \quad I_9 \equiv \int_0^{\infty} \frac{K}{df/d\eta} (2\eta)^j d\eta \quad (17)$$

and then substituting Eqs. 3 and 13 into it. The result for unconfined flow ( $dU/dx = 0$ ) is

$$\frac{\overline{u'v'}^*}{U^{*2}} = A_1 \frac{(2I_8/I_9)U^* + U}{(U^{*2} + UU^*)^{1/(j+1)}} \frac{d}{dx} (I_7 U^*) \quad (18)$$

with

$$A_1 \equiv - \frac{I_9}{I_5} \left( \frac{H}{I_1} \right)^{1/(j+1)} = \text{const.}$$

Several facts should be evident from this derivation. First, both  $I_7$  and  $I_8$  will in general vary slightly with  $x$ , because Eqs. 1 and 4a cannot be both valid except for the asymptotic range in which  $U^*/U \gg 1$ . Second, the ratio  $2I_8/I_9$  is smaller than unity and can be set equal to zero, if  $U^*/U \gg 1$ . Third, with  $\overline{u'v'}^*/U^*$  assumed constant, as is common practice in the conventional self-preservation approach, Eq. 18 yields the well-known power laws  $U^* \propto x^n$  for jets in stagnant fluid ( $U = 0$ ) as well as for wakes at large distances from the generating body ( $U^*/U \rightarrow 0$ ). For the general case, in which the parameter  $\overline{u'v'}^*/U^{*2}$  varies with  $x$ , on the other hand, Eq. 18 states the relationship between this variation and the function  $U^*(x)$ . It will be interesting to compare this relationship eventually with those found by Gartshore (1966) and Bradbury and Riley (1967), who have treated similar shear-stress parameters. Before this can be done, however, either  $U^*(x)$  must be known or two additional hypotheses have to be introduced for its evaluation.

The value of the complete analysis will ultimately depend on the degree to which analytical predictions agree with experimental data for a great variety of free-shear flows. It is for the purpose of making such comparison possible that mean-flow and turbulence measurements for various free-turbulence flows have been re-evaluated on the basis of the new similarity concept and are presented in the latter part of this paper. The comparison itself is left for a subsequent report. Suffice it here to note that a number of trials have shown that the prediction of the mean-flow development (i.e., the spreading  $\ell(x)$  of the diffusion zone and the decay  $U^*(x)$  of mean-velocity differences) seems to be rather insensitive to the particular content of the two additional hypotheses.



As long as the latter are used in conjunction with the new formulation of similarity, the mean-flow conditions appear to be adequately predicted, no matter whether, for example, the free-shear flow in question is considered as a columnar flow within a coaxial uniform stream which differs from its counterpart without superposed stream merely by the convective influence of that stream (Naudascher 1967), or the structure of the turbulent motion and its interdependence with the mean flow is regarded in analogy to the molecular motion by means of an eddy viscosity. This preliminary finding strongly suggests that the new similarity concept is physically sound.

The ultimate goal of this study, namely the prediction through a unified analysis of the developments of different types of free-shear flows, may well turn out not to be achievable unless the hypotheses on the turbulence structure take account of the effects of flow history as well as of local flow conditions. Whatever these hypotheses might be, however, the exploratory investigations seem to indicate that just as essential as the proper choice of these hypotheses is their use in combination with the new, more general form of self-preservation.

#### EXPERIMENTAL RESULTS

In order that experimental data can be evaluated in terms of the parameters introduced with the new assumptions of self-preservation (Eqs. 1, 2, and 5), one must first select appropriate definitions of the various dynamic and length scales involved. Because these scales are to be representative of the cross-sectional values of the corresponding dynamic characteristics and of the lateral extent over which they vary, it is most advantageous to use integral expressions for their determination. In accordance with the form chosen for  $P^*$  and  $\tau^*/\rho \equiv \overline{u'v'}$  (Eqs. 14 and 15), the following definitions are adopted in this paper:

$$q^{*2} \equiv \int_0^{\infty} (\overline{u'^2} + \overline{v'^2} + \overline{w'^2}) \left(\frac{2y}{\ell}\right)^j \frac{dy}{\ell} \quad (19)$$

$$u^{*2} \equiv \int_0^{\infty} \overline{u'^2} \left(\frac{2y}{\ell}\right)^j \frac{dy}{\ell} \quad (20)$$

Only  $U^*$  has not been determined from an integral relationship, i.e.,

$$U^* \equiv U_d \quad (21)$$

where  $U_d$  is the maximum mean-velocity difference (see Fig. 1). The values of  $U^*$  are hence more affected by inaccuracies in measurements than those of the other dynamic scales -- a fact which must be kept in mind in the interpretation of results.

Whenever possible, the length scale or effective width  $\ell$ , used in the evaluation of the dynamic scales (Eqs. 14, 15, 19, and 20), was obtained from

$$\ell_M^{j+1} \equiv \int_0^\infty \frac{\bar{u}_d^2 + U\bar{u}_d}{U^{*2} + UU^*} (2y)^j dy, \quad (20)$$

the significance of which is evident from the momentum equation. A simpler definition, i.e., the value  $y = y_{1/2}$  at which  $\bar{u}_d = \frac{1}{2}U_d$ , had to be adopted in evaluating  $q^*$  and  $\overline{u'v'}$  for Townsend's data (Table 1) and  $P^*$  from Bradbury's measurements (Fig. 14). The values of  $\ell_M$  presented in Table 1b for a round jet with  $U_j/U_0 = 1.48$ , moreover, must be used with caution, because the negative portions of the  $\bar{u}_d$  profiles near the edge of the diffusion zone, which were quite substantial in that case, were disregarded in the evaluation of Eq. 22.

Some of the data re-evaluated in this manner are listed in Table 1, the rest is displayed in Figs. 2 through 17. The parameter  $m$  is used to describe quantitatively the conditions of flow generation. For an unconfined stream, it is defined as

$$m \equiv \frac{2H}{U_0^2 R^{j+1}} = \frac{M_0}{\rho \pi^j R^{j+1} U_0^2} - \frac{Q_0}{\pi^j R^{j+1} U_0} \quad (23)$$

in which  $R$  is the half-width of the flow-generating body or jet (see Fig. 1),  $M_0$  is the excess momentum flux, and  $Q_0$  the excess volume flux produced at the flow origin. (For wakes of towed bodies,  $m$  is equal to minus one-half the drag coefficient,  $m = -C_D/2$ , whereas for wakes of self-propelled bodies,  $m = 0$ .) The quantity  $m$  is obviously better suited for a characterization of the investigated shear flows than, for example, the ratio of the jet-centerline velocity to the ambient-stream velocity,  $U_j/U_0$ , at the section of the jet exit.

It will be noted that the mean-flow characteristics attain similarity much more rapidly than turbulence characteristics (compare, e.g., Figs. 2 and 3 with 9 and 12) and that they seem to be self-preserving irrespective of the similarity assumptions employed. It must not be overlooked, however, that the

latter is only true because a different length scale, namely,

$$\ell_a^{j+1} \equiv \int_0^\infty \frac{\bar{u}_d}{U^*} (2y)^j dy \quad (24)$$

has been used in the representation of the velocity-difference profiles  $\bar{u}_d/U_d = g(y/\ell)$  in Figs. 2, 4, and 6. As seen in Fig. 13,  $\ell_M$  and  $\ell_Q$  do not grow in proportion to one another except, possibly, very far downstream from the flow origin. For any given choice of  $\ell$ , therefore, the  $f$  and  $g$  profiles (Eqs. 1 and 4a) cannot be both independent of  $x$ , and all integrals containing  $f$  as well as  $g$  can, at most, assume constant values asymptotically as  $U^*/U$  becomes very small.

It has been pointed out earlier (Naudascher 1967) that for axisymmetric jets in coaxial streams the  $f$  profiles are closer to a Gaussian distribution than the  $g$  profiles. The results of a recent investigation depicted in Figs. 2 and 3 verify this finding. For wake flows, for which  $\bar{u}_d$  as well as  $U_d$  assume negative values, on the contrary, both the  $f$  and  $g$  profiles appear to be equally far from a Gaussian distribution, as seen from a comparison of Figs. 4 and 5 and of Figs. 6 and 7. By comparing Figs. 4 and 6 or Figs. 5 and 7, on the other hand, one will note a definite dependence of the shape of the self-preserving profile on the conditions of flow generation. This persistence of peculiar features of the mean-velocity profiles, which are evidently associated with the distinct conditions of flow establishment, has also been reported by Reichardt and Ermshaus (1962) and explains, in part, the difference in the distributions of the turbulence-production parameter in Figs. 10 and 11 as well as the difference in the development of  $P^*\ell/U_d^3$  for different wake flows in Fig. 14. The excessive deviation from the similarity profile of the data for  $x/R = 6$  in Fig. 11 is due to the fact that the  $(\overline{u'^2} - \overline{v'^2})$  term in the momentum equation has a strong influence in the near-wake of a blunt body and must therefore be considered (see Carmody 1963, Fig. 13).

Figures 8 through 11 indicate that the similarity assumption expressed by Eq. 5 is well justified. The inconsistent deviations from the assumed similarity profile in Fig. 11 can probably be attributed to the lack of a common procedure for the reduction of reported and unreported data from test series with a 2-inch and a 6-inch disk.

From the logarithmic representation of the spreading of the diffusion zone in Fig. 13 it is clear that axisymmetric jets in coaxial streams do not spread in proportion to the  $1/3$ -power of the axial distance  $x$ , as the conventional self-preservation analysis would predict. If a power law can be used at all to describe the variation of  $\ell(x)$ , it appears to be closer to  $\ell \propto x^{2/3}$ . An estimate of the corrections which must be applied to Ortega's data (1968) for  $U_j/U_0 = 1.48$  (see footnote in Table 1) has yielded a decrease in the corresponding  $\ell_M$  values of almost inverse proportion with respect to  $x$ ; when plotted in Fig. 13, the corrected  $\ell_M$  values would therefore show a rate of growth that is comparable to that of the other jet-flow data.

The downstream development of other significant flow parameters is represented in Figs. 14 through 17. The use of  $U/U_d$  instead of  $x/R$  in these figures serves the purpose of facilitating future comparison with analytical predictions and checking the validity of the basic supposition, made in most investigations of free-shear flows, that far downstream such flows become independent of the precise flow conditions at the origin or, in other words, they become describable in terms of such local flow characteristics as  $U/U_d$ . Evidently, this assumption does not hold for wakes. Behind a blunt body, any of the parameters depicted in Figs. 14, 15, and 16 seem to be larger by about an order of magnitude than the corresponding parameters for a wake behind a slender body. Even jet flows do not seem to be quite free of an influence of the flow origin, if the trend of the curves in Fig. 16 is any indication. It may well be, however, that  $\overline{u'^2}/U_d^2$  is not a good indicator of conditions at a given cross-section. As already mentioned, integral expressions such as  $u^{*2}$  or  $\overline{u'v'^*}$  are much more preferable in this regard than local values such as  $\overline{u'^2}$  or  $U_d$ , because the latter are affected by both inaccuracies of measurement and deviations from the similarity profiles.

It is for this reason that more weight should be given to the  $\overline{u'v'^*}/u^{*2}$  data in Fig. 17. Their constancy for any one jet flow is an important finding, one that may well be utilized in future analytical work. Whether this constancy is a general characteristic of free-turbulence shear flows cannot, of course, be postulated before comparable data are derived from plane-jet and wake measurements. The trend of the  $\overline{u'v'_{\max}}/\overline{u'^2}$  data is inconclusive in this regard as seen from a comparison of the corresponding data of Curtet and Ricou (Fig. 17).

Much work needs still to be done before the interrelationship between mean flow and turbulence is completely understood. For example, it will be interesting to learn whether the discrepancy in magnitude and trend between the wake-data of Carmody (1963) and those by Cooper and Lutzki (1955), shown in Fig. 16, are due to deficiencies in measurement techniques or errors in data reduction; it is hardly conceivable that the wake behind a disk could have characteristics that are so drastically different from those of the wake behind a square plate, considering the insignificant difference in Reynolds numbers (35,000 versus 16,300).

Data for a wake of a self-propelled body are included in Fig. 16, because this flow represents the limiting case of jet flow for  $m \rightarrow 0$ . As a matter of fact, Ortega's test series with  $U_j/U_0 = 1.48$  and  $m \approx 0.07$  was very close to this limit due to the relatively large wake effect produced by the resistance of the jet-supplying pipe.\* The convection rate of turbulence energy in this case may well be as important as it was shown to be for the wake of a self-propelled body (Naudascher 1965), so that the simplifications of the momentum and energy equations used in the preceding chapter may no longer apply (see Naudascher 1965 and 1967 for a separate analysis of this particular flow). It is interesting to point out in this context that the two curves in Fig. 16 for almost equal values of  $U_j/U_0$  (2.03 versus 2.0) but different  $m$  show divergent trends.

A basis for the most critical test on the validity of the required two hypotheses and thus on the validity of the complete similarity analysis is provided by the data in Figs. 14 and 15.\*\* Unfortunately, such data are not easy to obtain, because not only does the procedure of evaluation demand great precision and time-consuming calculations, but much of the necessary information is often not available. In Fig. 14, for example, points for the data of Bradbury and Riley (1967) had to be determined using  $l \equiv y_{1/2}$  rather than  $l \equiv l_M$

---

\*It should be noted that the small value of  $m$  in this case was caused by a partial cancellation of jet thrust by the drag of the pipe. In contrast hereto, the magnitude of  $m$  for wakes past slender-bodies is limited merely by the low value of drag coefficient. The turbulence in the wake is therefore subject to a relatively higher rate of strain and must be expected to have a different structure than the turbulence in the jet-flow counterpart.

\*\*Note that in contrast to Fig. 13 of the preceding report (Naudascher 1967), the data in Figs. 14 and 15 are all based on turbulence rather than mean-flow measurements.

as in all other cases, and assuming a constant value  $I' = 1.0914$  in the expression for the eddy Reynolds number (see Eq. 5 of their paper). The limitations of Ortega's measurements for  $U_j/U_0 = 1.48$  have already been stated; only his two last points, for which the neglected outer portions of the momentum and shear profiles have little influence on the evaluated parameters, are therefore included in Figs. 14 and 15. Yet, even they may be in error because of the relatively high level of background turbulence.

In spite of these limitations, Figs. 14 and 15 prove beyond doubt that the conventional similarity assumptions (Eqs. 4) do not apply to wakes and jets in coaxial streams, at least not within the range of practical interest. For axisymmetric jet flows, moreover, one cannot even speak of an asymptotic tendency toward self-preservation of the conventional type, as both  $P^*l/U_d^3$  and  $\overline{u'v'}^*/U_d^2$  appear to grow monotonically with increasing  $U/U_d$  and, thus, with  $x$ .

Whether this growth is indeed independent of the conditions of jet-flow establishment, as the plotted data suggest, cannot be concluded with certainty. After the experience gained with the use of different definitions for the other dynamic scales, it would seem that the generality of the relationships in Figs. 13 through 17 could be augmented by replacing  $U^* \equiv U_d$  and  $l \equiv l_M$  by scales derived from integral expressions, such as for example,

$$U^* l^{j+1} \equiv \int_0^{\infty} \bar{u}_d (2y)^j dy \quad (25a)$$

$$(U^{*2} + UU^*) l^{j+1} \equiv \int_0^{\infty} (\bar{u}_d^2 + U\bar{u}_d) (2y)^j dy \quad (25b)$$

According to these equations,  $U^*$  and  $l$  would be equivalent to the mean excess velocity and width of a columnar flow (flow with top-hat profiles), a flow which satisfies the continuity and momentum conditions.

#### CONCLUSIONS

Even though a complete analytical solution for the development of plane and axially symmetric free-turbulence flows has not yet been found, a significant confirmation on the validity of a new similarity concept was obtained by the observation that different hypotheses on the turbulence structure

all lead to satisfactory predictions of the mean-flow field when based on the new similarity assumptions. For a continuation of the analytical work it proved to be necessary to re-evaluate experimental data on a great variety of free-turbulence flows on the basis of the new similarity concept and to use them for an examination of the interrelationship between mean-flow and turbulence and, ultimately, for the formulation of a reasonable hypothesis on the turbulence structure.

The results of this endeavor have contributed additional confirmation on the validity of the new similarity analysis. The distributions of mean-flow as well as turbulence characteristics in various wake and jet flows were found to conform very satisfactorily to the postulated similarity laws except very close to the flow origins; and both the spreading of these flows and the downstream development of ratios of turbulence to mean-flow velocity scales were found to differ appreciably from the predictions obtained by using the conventional similarity assumptions. In regard to the common notion that free-shear flows become independent of the precise flow conditions at the origin, the results are conflicting. Whereas there seems to exist a definite dependence on such conditions of both the form of lateral distributions and the trend of axial developments of wake-flow parameters, jet flows appear to behave more nearly in agreement with this notion.

While the experimental evidence presented in this paper does provide the desired insight into the interdependence of mean and turbulent motion, more needs to be done before a unified treatment of inhomogeneous free-turbulence flows can be attempted with the new similarity analysis. First, the generality of the proportional development of  $\overline{u'v'}$  and  $u'^2$  must be checked for plane-jet and wake flows; second, the difference between the rates of decay of turbulence and mean-flow velocity scales in plane wakes needs to be studied with the aim of testing Townsend's results, which are in contrast even regarding the overall trend to the present findings for various axisymmetric free-shear flows; third, the validity of the simplifications in the equations of motion is to be clarified for the critical case of a jet-wake combination with relatively small excess momentum flux by means of a turbulence-energy balance; and, fourth, the influence of replacing  $U_d$  by a more representative mean-velocity scale should be examined for all cases. More reliable experimental information on the growth of  $\lambda$  with  $x$  would also be helpful.

ACKNOWLEDGEMENT

Most of the calculations required in the evaluation of the presented data were performed by T. H. Yoon, Research Associate of the Iowa Institute of Hydraulic Research.



REFERENCES

- Bradbury, L. J. S., and Riley, J., 1967, "The Spread of a Turbulent Plane Jet Issuing into a Parallel Moving Airstream," *J. Fluid Mech.*, vol. 27, 381.
- Carmody, T., 1963, "Establishment of the Wake Behind a Disk," Ph.D. Dissertation, University of Iowa, (see also *ASME J. Basic Eng.*, Dec. 1964, 869).
- Chevray, R., 1967, "The Turbulent Wake of a Body of Revolution," Ph.D. Dissertation, University of Iowa, (See also *ASME J. Basic Eng.*, Paper No. 68-FE-16).
- Cooper, R. D., and Lutzky, M., 1955, "Exploratory Investigation of the Turbulent Wakes Behind Bluff Bodies," R. & D. Report 963, David Taylor Model Basin.
- Curtet, R., and Ricou, F. P., 1964, "On the Tendency to Self-Preservation in Axisymmetric Ducted Jets," *ASME J. Basic Eng.*, 765.
- Gartshore, I. S., 1966, "An Experimental Examination of the Large-Eddy Equilibrium Hypothesis," *J. Fluid Mech.*, vol. 29, 89.
- Kruka, V., and Eskinazi, S., 1964, "The Wall Jet in a Moving Stream", *J. Fluid Mech.*, vol. 29, 555.
- Naudascher, E., 1965, "Flow in the Wake of Self-Propelled Bodies and Related Sources of Turbulence," *J. Fluid Mech.*, vol. 22, 625.
- Naudascher, E., 1967, "On a General Similarity Analysis for Turbulent Jet and Wake Flows," IIHR Report No. 106, Iowa Institute of Hydraulic Research, Iowa City, Iowa.
- Ortega, J. J., 1968, "Characteristics of a Turbulent Round Jet in a Coaxial Stream," M.S. Thesis, University of Iowa.
- Reichardt, H., and Ermshaus, R., 1962, "Impuls- und Warmetubertragung in turbulenten Windschatten hinter Rotationskorpern," *Int. J. Heat Mass Transfer*, vol. 5, 251.
- Rouse, H., 1960, "Distribution of Energy in Regions of Separation," *La Houille Blanche* no. 3/4.
- Sami, S., Carmody, T., and Rouse, H., 1967, "Jet Diffusion in the Region of Flow Establishment," *J. Fluid Mech.*, vol. 27, 231.
- Townsend, A. A., 1948, "Local Isotropy in the Turbulent Wake of a Circular Cylinder," *Aust. J. Sci. Res.*, vol. 12, 451.
- Townsend, A. A., 1949, "Momentum and Energy Diffusion in the Turbulent Wake of a Cylinder," *Proc. Roy. Soc.*, vol. 197, 124.
- Townsend, A. A., 1956, *The Structure of Turbulent Shear Flows*, Cambridge University Press.

Table 1. Flow parameters for various jet and wake flows.

(a) Curtet & Ricou (1964), round jet in a coaxial stream.

$U_j/U_0 = 3.72$   
 $m = 9.45$

$\frac{x}{R}$	$\frac{U}{U_m}$	$\frac{U}{U_d}$	$\frac{\overline{u'^2}}{U_d^2}$	$\frac{u^{*2}}{U_d^2}$	$\frac{\overline{u'v'^*}}{U_d^2}$	$\frac{P^* \ell_M}{U_d^3}$	$\frac{\overline{u'v'^*}}{\overline{u'^2}}$	$\frac{\overline{u'v'^*}}{u^{*2}}$	$\frac{\overline{u'v'_{max}}}{\overline{u'^2}}$
10	0.9837	0.368	0.0010	0.0407	0.0120	0.0086	12.0	0.295	7.08
20	0.9795	0.426	0.0202	0.0755	0.0183	0.0099	0.905	0.242	0.46
30	0.9753	0.597	0.0380	0.103	0.0236	0.0133	0.616	0.229	0.37
40	0.9726	0.791	0.0480	0.118	0.0265	0.0152	0.552	0.225	0.315
50	0.9716	1.002	0.0535	0.127	0.0286	0.0169	0.535	0.225	0.305
60	0.9716	1.218	0.0568	0.134	0.0311	0.0186	0.548	0.232	0.31
75	0.9747	1.576	0.0640	0.142	--	--	--	--	--
90	0.9800	1.949	0.0720	0.150	0.0365	0.0222	0.507	0.243	0.265

$U_j/U_0 = 2.03$   
 $m = 1.53$

$\frac{x}{R}$	$\frac{U}{U_m}$	$\frac{U}{U_d}$	$\frac{\overline{u'^2}}{U_d^2}$
10	0.9963	0.982	0.0010
20	0.9942	1.063	0.0144
30	0.9942	1.408	0.0352
40	0.9952	1.789	0.0448
50	0.9963	2.279	0.0564
60	0.9989	2.756	0.0649
75	1.0036	3.492	0.0694
90	1.0105	4.304	0.0753

$U_j/U_0 = 5.56$   
 $m = 24.1$

$\frac{x}{R}$	$\frac{U}{U_m}$	$\frac{U}{U_d}$	$\frac{\overline{u'^2}}{U_d^2}$
10	0.9668	0.216	0.0008
20	0.9574	0.256	0.0169
30	0.9474	0.363	0.0316
40	0.9395	0.483	0.0376
50	0.9337	0.618	0.0470
60	0.9295	0.751	0.0529
75	0.9274	0.962	0.0584
90	1.9290	1.170	0.0613

(b) Ortega (1968), round jet in a coaxial stream ( $U = \text{const}$ ).\*

$U_j/U_0 = 2.00$   
 $m = 0.93$

$\frac{x}{R}$	$\frac{U}{U_d}$	$\frac{\overline{u'^2}}{U_d^2}$	$\frac{u^{*2}}{U_d^2}$	$\frac{\overline{u'v'^*}}{U_d^2}$	$\frac{P^* \ell_M}{U_d^3}$	$\frac{\overline{u'v'^*}}{\overline{u'^2}}$	$\frac{\overline{u'v'^*}}{u^{*2}}$	$\frac{\ell_M}{R}$	$\frac{y_{1/2}}{R}$
24	1.44	0.0165	0.0971	0.0268	0.0159	1.625	0.276	0.865	0.865
60	3.52	0.0610	0.1470	0.0450	0.0346	0.737	0.306	1.58	1.53
96	6.12	0.0873	0.2040	0.0570	0.0448	0.653	0.279	2.19	2.04
144	10.10	0.1118	0.3380	0.0915	0.0710	0.818	0.271	2.69	2.44
192	13.85	0.1700	0.4210	0.1250	0.0958	0.735	0.297	3.30	2.92

$U_j/U_0 = 1.48$   
 $m = 0.07^*$

$\frac{x}{R}$	$\frac{U}{U_d}$	$\frac{\overline{u'^2}}{U_d^2}$	$\frac{u^{*2}}{U_d^2}$	$\frac{\overline{u'v'^*}}{U_d^2}$	$\frac{P^* \ell_M}{U_d^3}$	$\frac{\overline{u'v'^*}}{\overline{u'^2}}$	$\frac{\overline{u'v'^*}}{u^{*2}}$	$\frac{\ell_M}{R}$	$\frac{y_{1/2}}{R}$
24	3.80	0.0448	0.158	0.0578	0.0448	1.290	0.366	0.615	0.60
60	10.55	0.1082	0.281	0.1005	0.0906	0.929	0.358	1.00	0.96
96	21.12	0.2220	0.480	0.1810	0.1509	0.815	0.377	1.26	1.12
132	40.00	0.4460	0.840	0.3200	0.2591	0.717	0.380	1.38	1.20

\*Ortega's  $\ell_M$ ,  $u^*$ ,  $\overline{u'v'^*}$ , and  $P^*$  data for  $U_j/U_0 = 1.48$  are affected by the neglect of negative  $\overline{u_d}$  and  $\overline{u'v'}$  values near the edge of the diffusion zone and by a relatively high level of background turbulence.

(c) Chevray (1967), wake of a slender spheroid.  $UR/\nu = 1,375,000$ ;  $m = -0.03$ .

$\frac{x}{R}$	$\frac{U}{U_d}$	$\frac{\overline{u'^2}}{U_d^2}$	$\frac{q^{*2}}{U_d^2}$	$\frac{\overline{u'v'^*}}{U_d^2}$	$\frac{\overline{u'v'_{max}}}{U_d^2}$	$\frac{P^* \ell_M}{U_d^3}$	$\frac{\overline{u'v'^*}}{\overline{u'^2}}$	$\frac{\overline{u'v'_{max}}}{\overline{u'^2}}$	$\frac{\ell_M}{R}$	$\frac{\ell_Q}{R}$
2	2.02	0.0040	--	0.0028	--	0.0024	0.70	--	0.43	0.356
6	2.74	0.0070	--	0.0073	0.0055	0.0046	1.047	0.79	0.39	--
12	3.64	0.0144	0.083	0.0165	0.0109	0.0112	1.145	0.76	0.405	0.375
18	5.13	0.0278	0.172	0.0345	0.0223	0.0262	1.241	0.80	0.435	0.415
24	6.53	0.0435	0.234	0.0516	0.0335	0.0472	1.184	0.77	0.485	0.465
30	8.47	0.0584	0.354	0.0666	0.0421	0.0527	1.140	0.72	0.535	0.52
36	10.53	0.0882	0.475	0.0668	0.0423	0.0593	0.757	0.49	0.605	0.60

(d) Carmody (1963), wake of a disk.  $UR/\nu = 35,000$ ;  $m = -0.57$ .

$\frac{x}{R}$	$\frac{U}{U_d}$	$\frac{\overline{u'^2}}{U_d^2}$	$\frac{\overline{u'v'^*}}{U_d^2}$	$\frac{\overline{u'v'_{max}}}{U_d^2}$	$\frac{P^* \ell_M}{U_d^3}$	$\frac{\overline{u'v'^*}}{\overline{u'^2}}$	$\frac{\overline{u'v'_{max}}}{\overline{u'^2}}$	$\frac{\ell_M}{R}$	$\frac{\ell_Q}{R}$
4	0.69	0.008	--	--	--	--	--	--	--
6	1.39	0.040	0.023	0.066	0.0289	0.575	1.65	2.08	1.43
8	2.82	0.184	0.109	0.109	0.0886	0.592	0.59	1.86	1.67
12	6.80	0.657	0.438	0.397	0.658	0.667	0.60	2.09	1.94
18	11.05	0.775	0.659	0.045	0.594	0.850	0.575	2.43	2.40
24	14.65	0.893	0.885	0.55 ?	0.816	0.991	0.615	2.77	2.83
30	18.65	0.941	--	0.49 ?	--	--	0.52	3.00	3.05

(e) Townsend (1956), wake of a circular cylinder.

$\frac{UR}{\nu} = 4050$

$\frac{x}{R}$	$\frac{U}{U_d}$	$\frac{q^{*2}}{U_d^2}$
160	8.96	0.80
240	10.69	0.52
320	12.22	0.47

$\frac{UR}{\nu} = 680$

$\frac{x}{R}$	$\frac{U}{U_d}$	$\frac{\overline{u'^2}}{U_d^2}$	$\frac{\overline{u'v'^*}}{U_d^2}$	$\frac{\overline{u'v'_{max}}}{\overline{u'^2}}$
1000	22.37	0.0815	0.694	0.635
1300	25.44	0.072	0.633	0.65
1600	39.40	0.074	0.665	0.69
1900	31.40	0.0715	--	--

(f) Naudascher (1965), wake of a self-propelled disk.  $UR/\nu = 27,500$ ;  $m = 0$ .

$\frac{x}{R}$	$\frac{U}{U_d}$	$\frac{\overline{u'^2}}{U_d^2}$	$\frac{\overline{u'v'_{max}}}{\overline{u'^2}}$
8	2.75	0.461	0.267
10	3.97	0.419	0.246
14	7.46	0.674	0.254
20	16.95	1.587	0.236
30	36.1	3.725	0.178
40	67.1	6.656	0.133
50	109.0	12.89	0.128

LIST OF FIGURES

- Fig. 1 Definition sketch.
- Fig. 2 Radial variation of mean-velocity difference in a round jet. (Data by Ortega for  $U_j/U_0 = 2.00$ ;  $m = 0.93$ .)
- Fig. 3 Radial variation of momentum parameter in a round jet. (Data by Ortega for  $U_j/U_0 = 2.00$ ;  $m = 0.93$ .)
- Fig. 4 Radial variation of mean-velocity difference in the wake of a slender spheroid. (Data by Chevray for  $UR/\nu = 1,375,000$ ;  $m = -0.03$ .)
- Fig. 5 Radial variation of momentum parameter in the wake of a slender spheroid. (Data by Chevray for  $UR/\nu = 1,375,000$ ;  $m = -0.03$ .)
- Fig. 6 Radial variation of mean-velocity difference in the wake of a disk. (Data by Carmody for  $UR/\nu \approx 35,000$ ;  $m = -0.57$ .)
- Fig. 7 Radial variation of momentum parameter in the wake of a disk. (Data by Carmody for  $UR/\nu \approx 35,000$ ;  $m = -0.57$ .)
- Fig. 8 Radial variation of turbulence-production parameter in a round jet. (Data by Curtet and Ricou for  $U_j/U_0 = 3.72$ ;  $m = 9.45$ .)
- Fig. 9 Radial variation of turbulence-production parameter in a round jet. (Data by Ortega for  $U_j/U_0 = 2.00$ ;  $m = 0.93$ .)
- Fig. 10 Radial variation of turbulence-production parameter in the wake of a slender spheroid. (Data by Chevray for  $UR/\nu = 1,375,000$ ;  $m = -0.03$ .)
- Fig. 11 Radial variation of turbulence-production parameter in the wake of a disk. (Data by Carmody for  $UR/\nu \approx 35,000$ ;  $m = -0.57$ .)
- Fig. 12 Radial variation of longitudinal turbulence intensity in a round jet. (Data by Ortega for  $U_j/U_0 = 2.00$ ;  $m = 0.93$ .)
- Fig. 13 Axial variation of effective width for various jet and wake flows.
- Fig. 14 Variation with  $U/U_d$  of  $P^*l/U_d^3$  for various jet and wake flows.
- Fig. 15 Variation with  $U/U_d$  of the ratio of a characteristic cross-sectional value of  $\overline{u'v'}$  to  $U_d^2$  for various jet and wake flows.

Fig. 16 Variation with  $U/U_d$  of the ratio of a characteristic cross-sectional value of  $\overline{u'^2}$  to  $U_d^2$  for various jet and wake flows.

Fig. 17 Variation with  $U/U_d$  of characteristic cross-sectional values of  $\overline{u'v'}/\overline{u'^2}$  for various jet and wake flows.

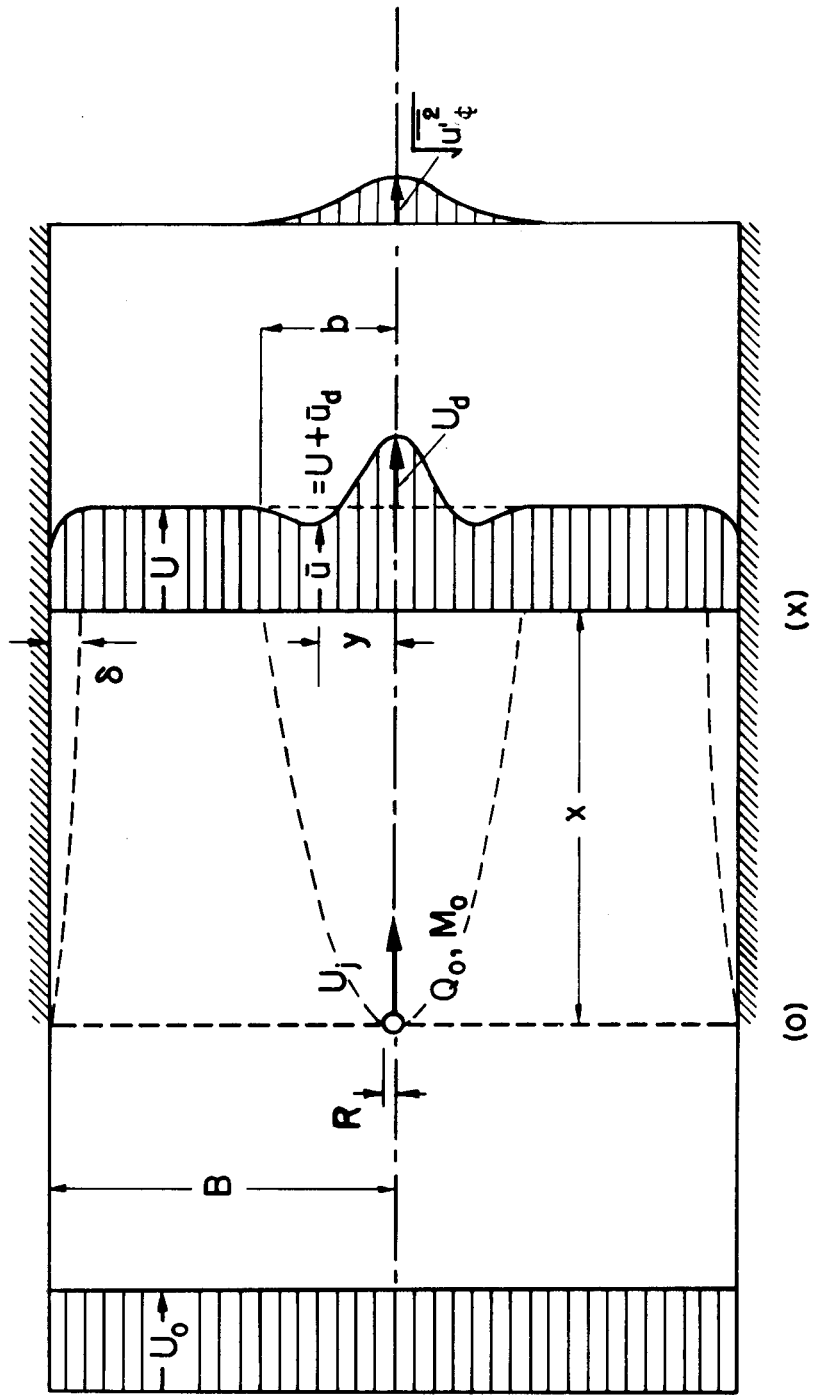


Fig. 1 Definition sketch.

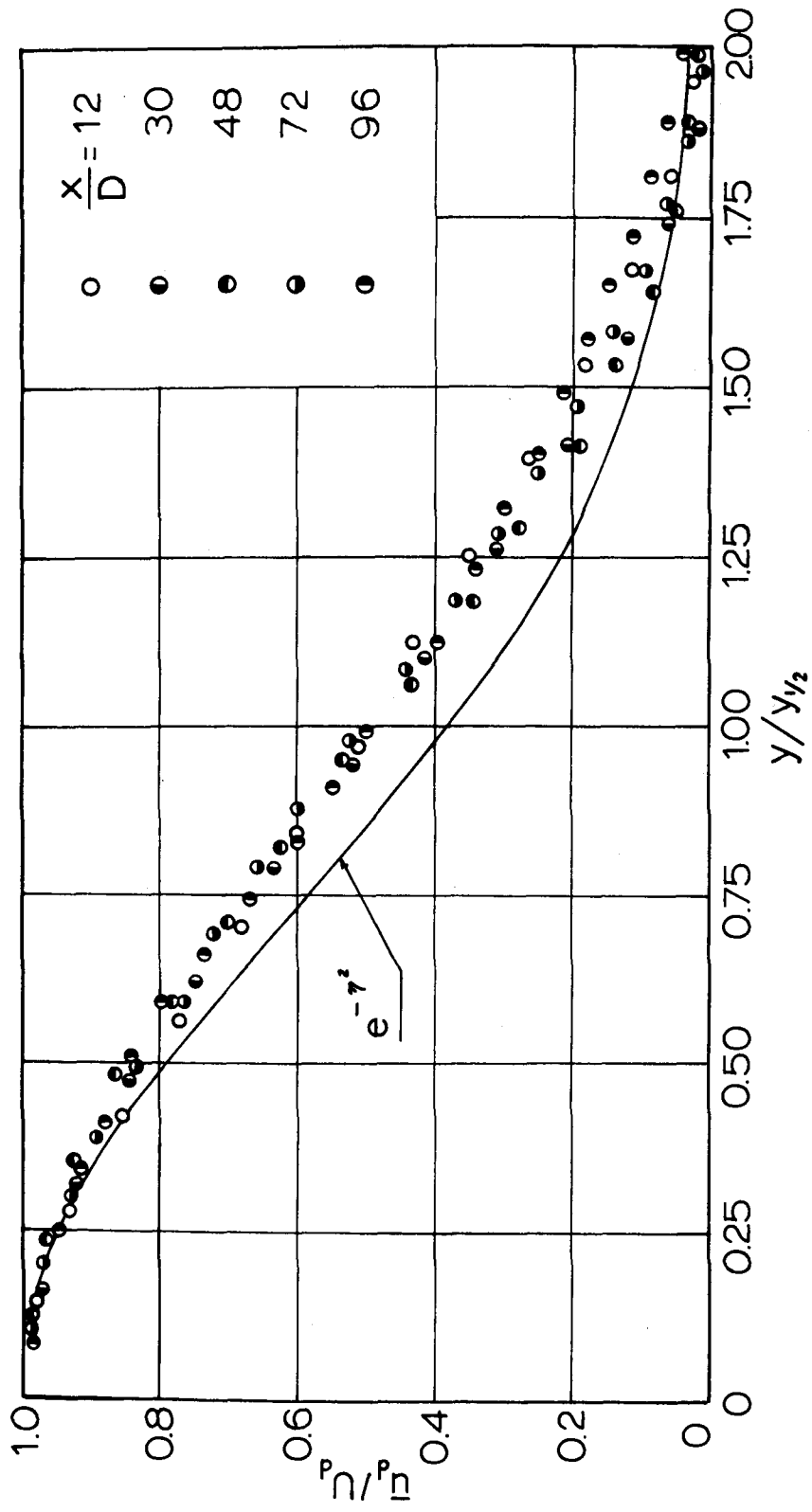


Fig. 2 Radial variation of mean-velocity difference in a round jet.  
 (Data by Ortega for  $U_j/U_0 = 2.00$ ;  $m = 0.93$ .)

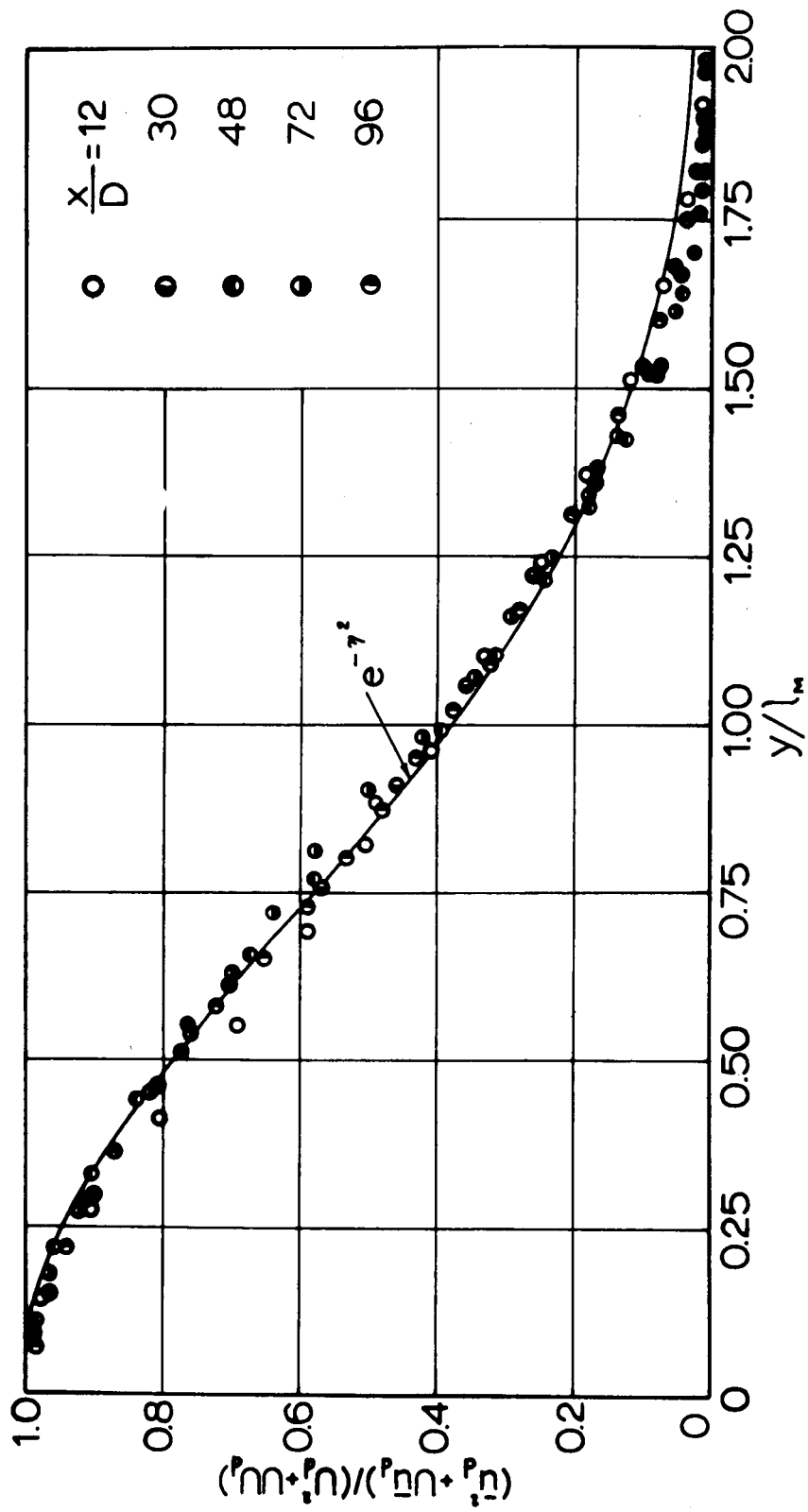


Fig. 3 Radial variation of momentum parameter in a round jet.  
 (Data by Ortega for  $U_j/U_0 = 2.00$ ;  $m = 0.93$ .)



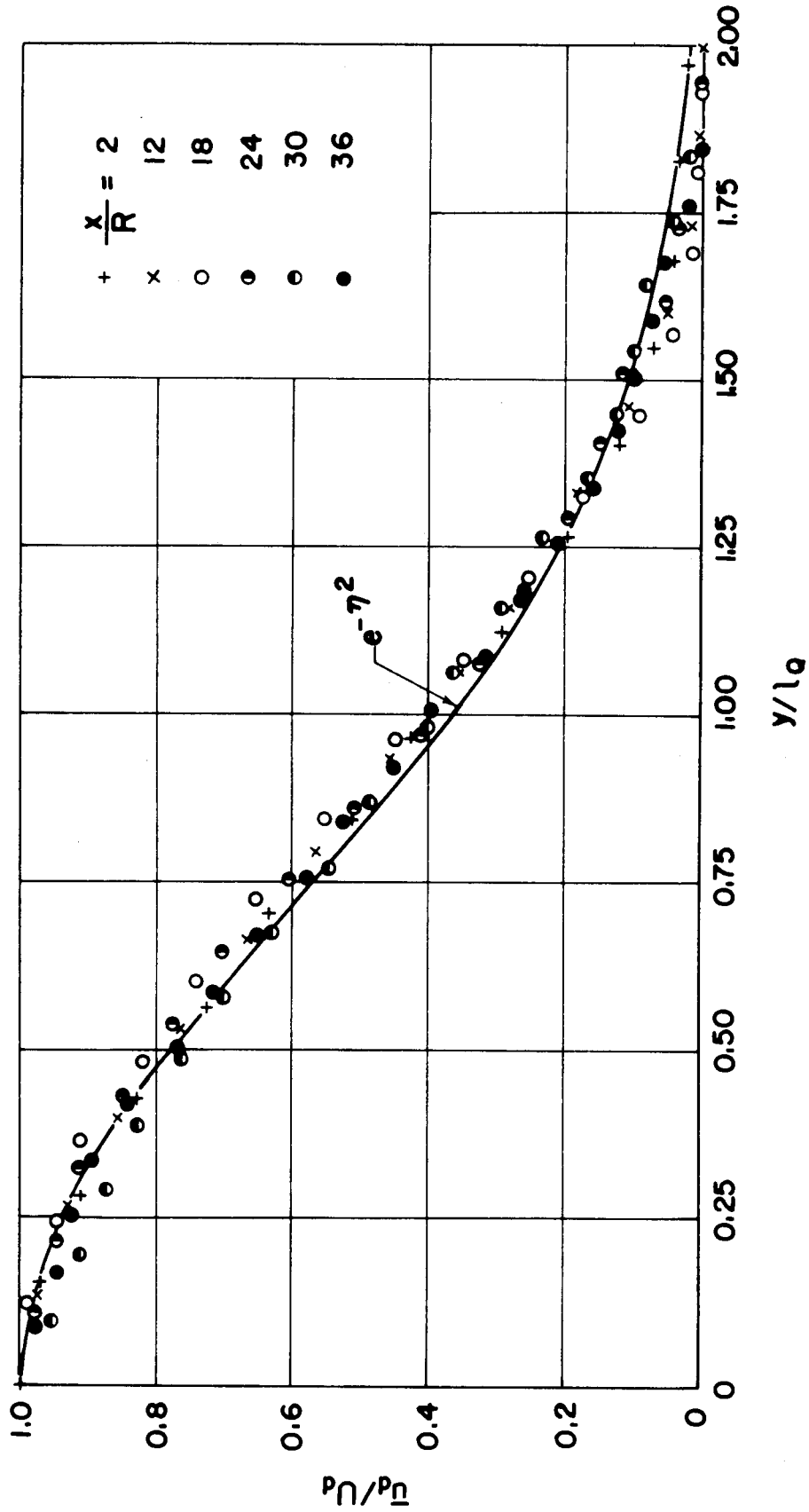


Fig. 4 Radial variation of mean-velocity difference in the wake of a slender spheroid.  
 (Data by Chevray for  $UR/\nu = 1,375,00$ ;  $m = -0.03$ .)

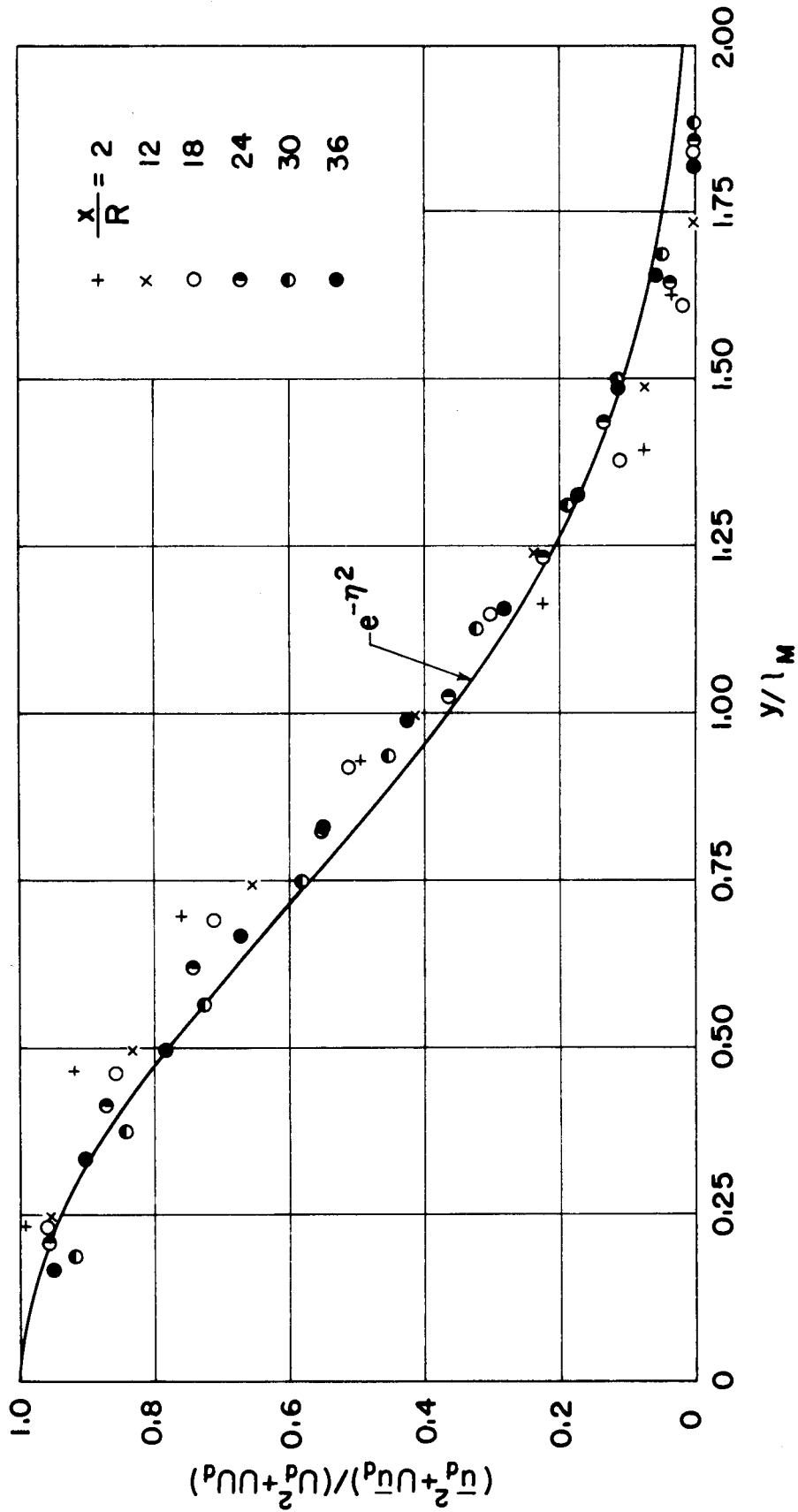


Fig. 5 Radial variation of momentum parameter in the wake of a slender spheroid.

(Data by Chevray for  $UR/\nu = 1,375,000$ ;  $m = -0.03$ .)

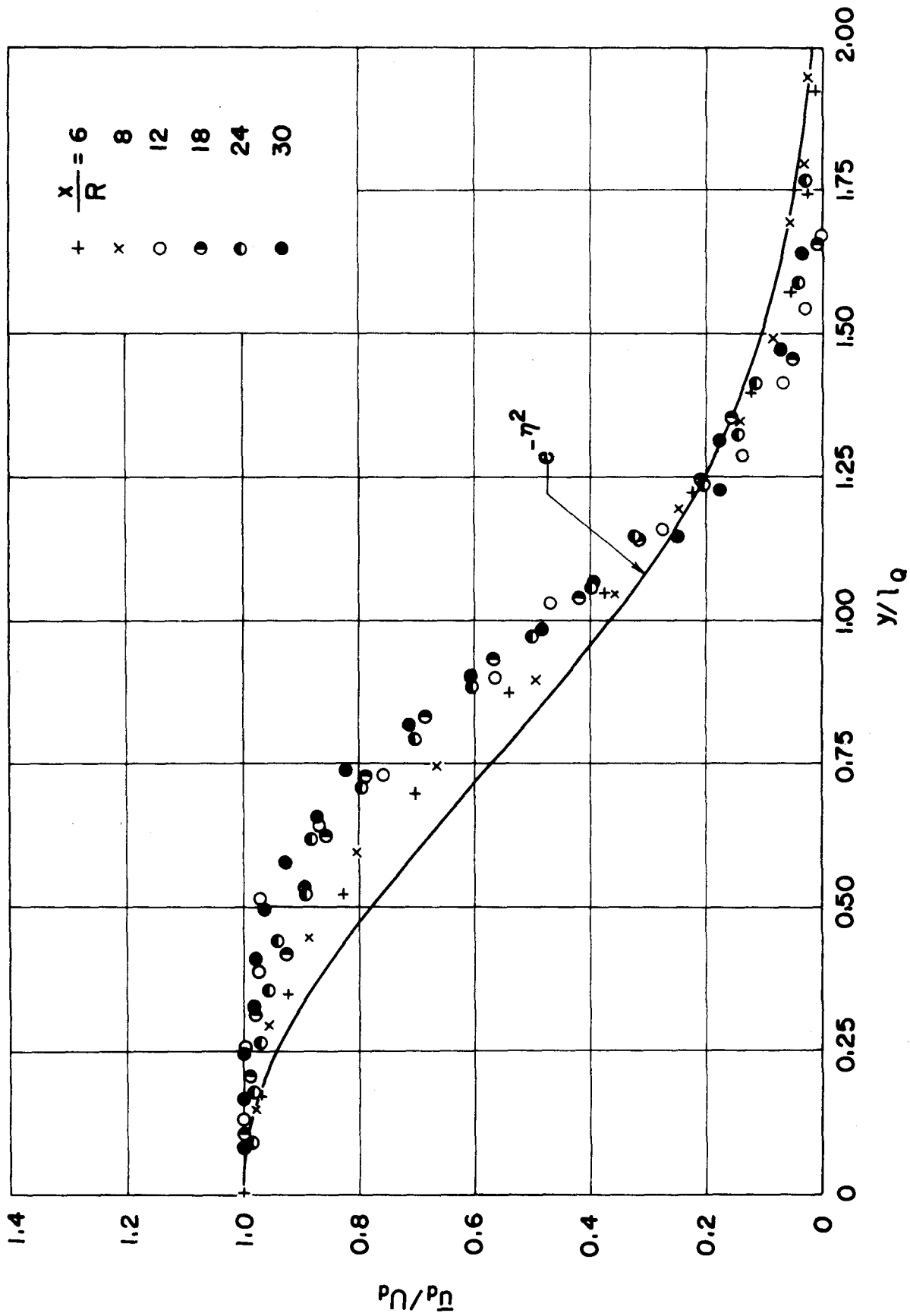


Fig. 6 Radial variation of mean-velocity difference in the wake of a disk.

(Data by Carmody for  $UR/\nu \approx 35,000$ ;  $m = -0.57$ .)

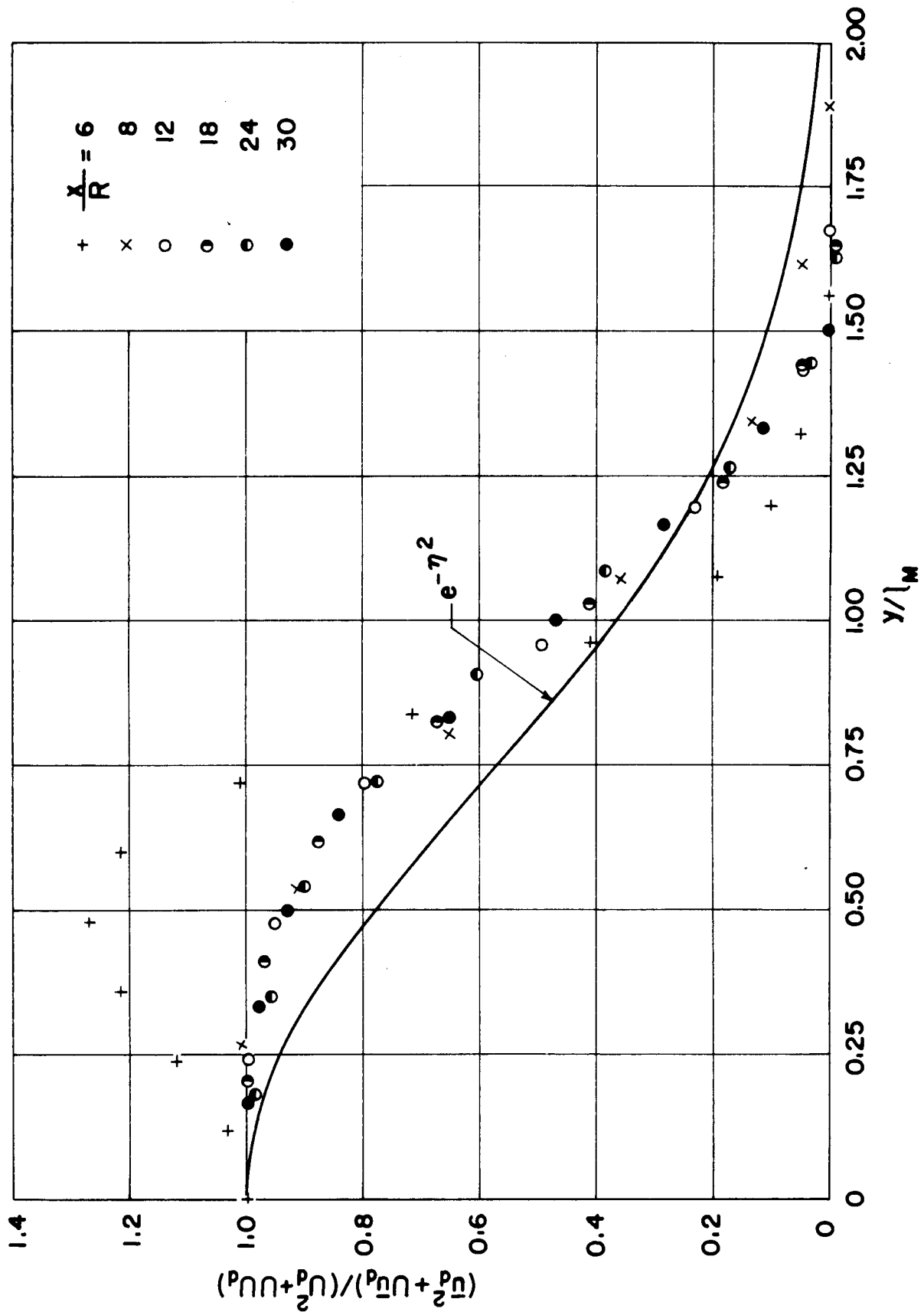


Fig. 7 Radial variation of momentum parameter in the wake of a disk.  
 (Data by Carmody for  $UR/\nu \approx 35,000$ ;  $m = -0.57$ .)

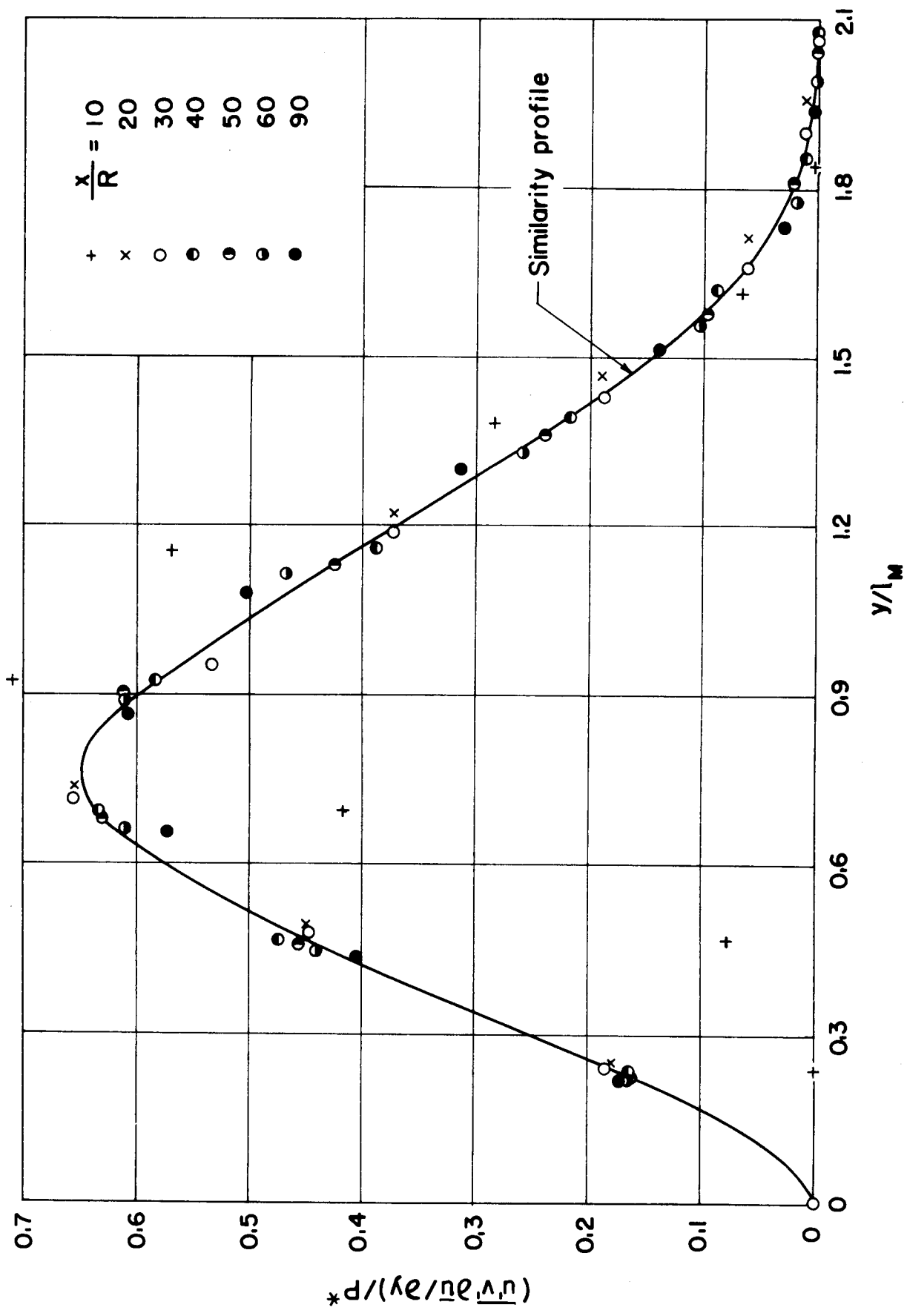


Fig. 8 Radial variation of turbulence-production parameter in a round jet.  
 (Data by Curtet and Ricou for  $U_j/U_0 = 3.72$ ;  $m = 9.45$ .)

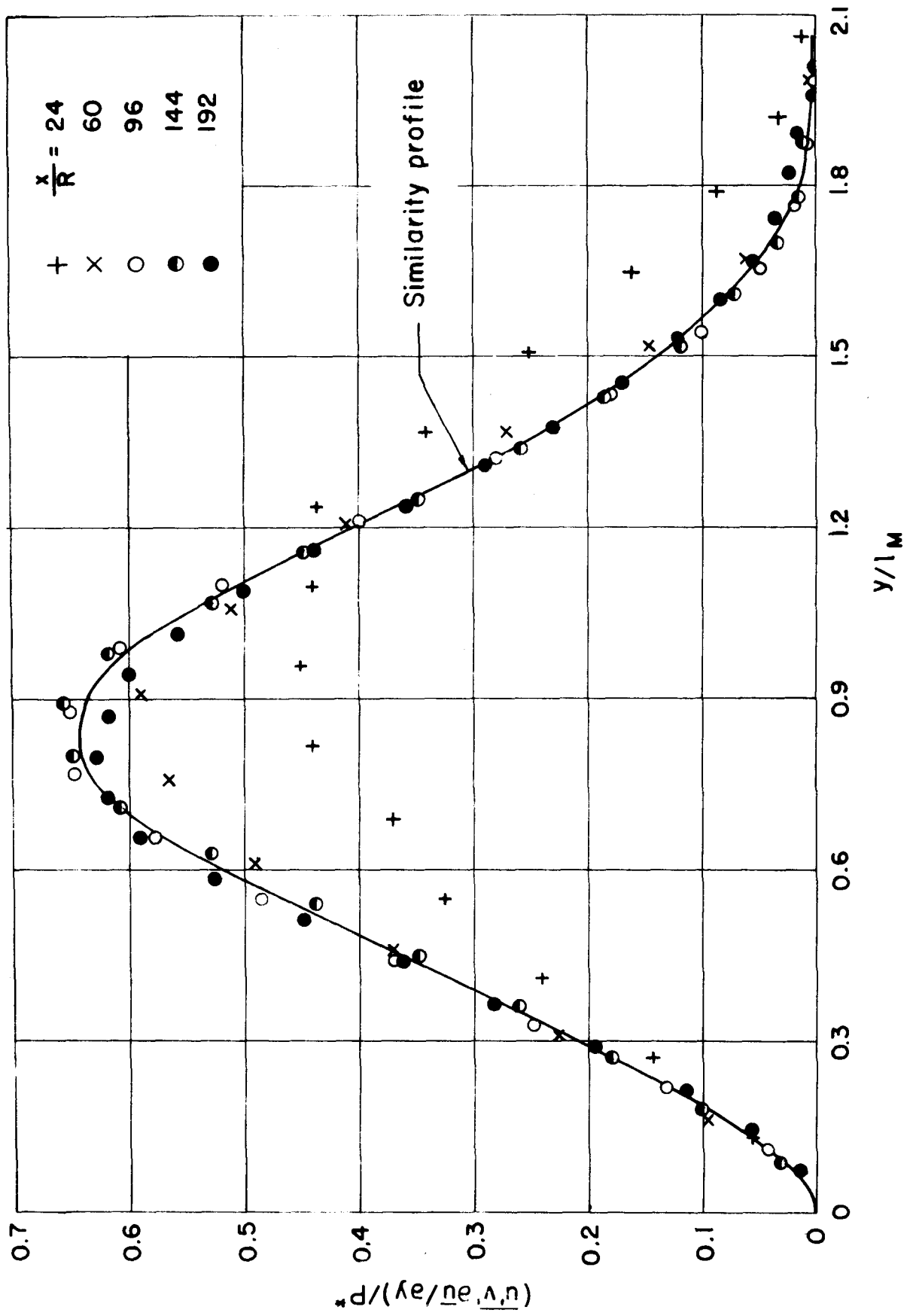


Fig. 9 Radial variation of turbulence-production parameter in a round jet.  
 (Data by Ortega for  $U_j/U_0 = 2.00$ ;  $m = 0.93$ .)

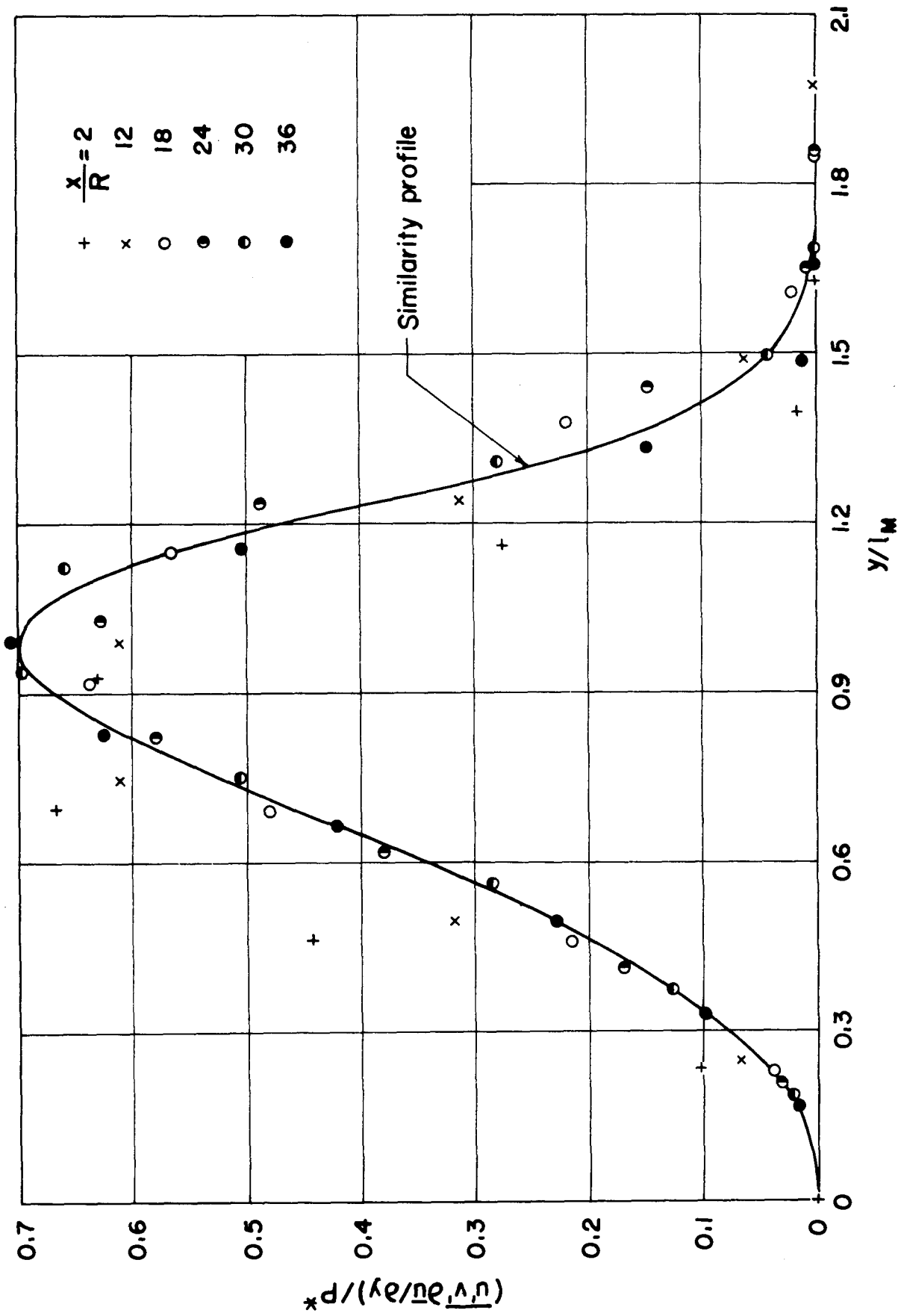


Fig. 10 Radial variation of turbulence-production parameter in the wake of a slender spheroid.  
 (Data by Chevray for  $UR/\nu = 1,375,000$ ;  $m = -0.03$ .)

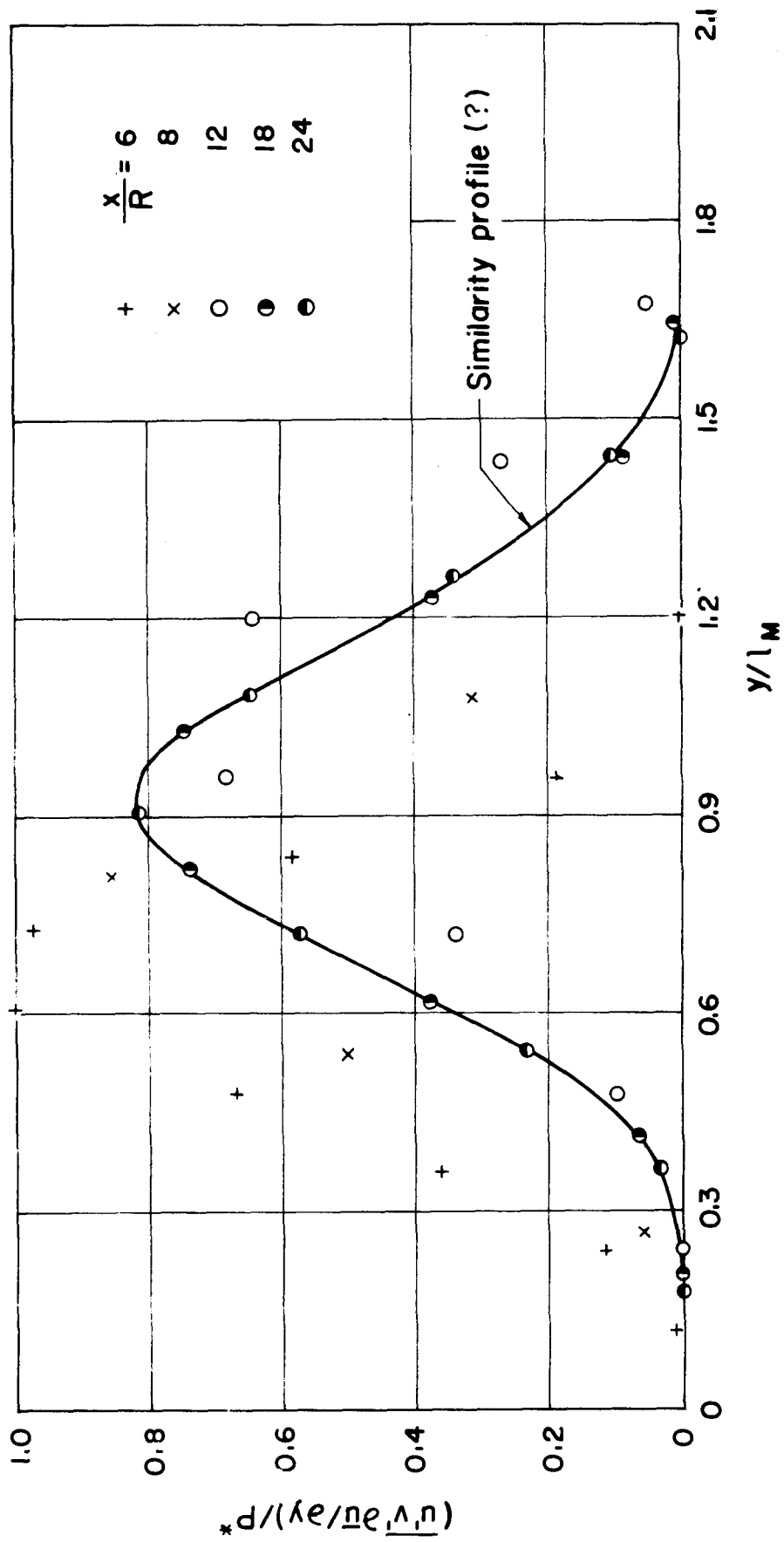


Fig. 11 Radial variation of turbulence-production parameter in the wake of a disk.  
 (Data by Carmody for  $UR/\nu \approx 35,000$ ;  $m = -0.57$ .)



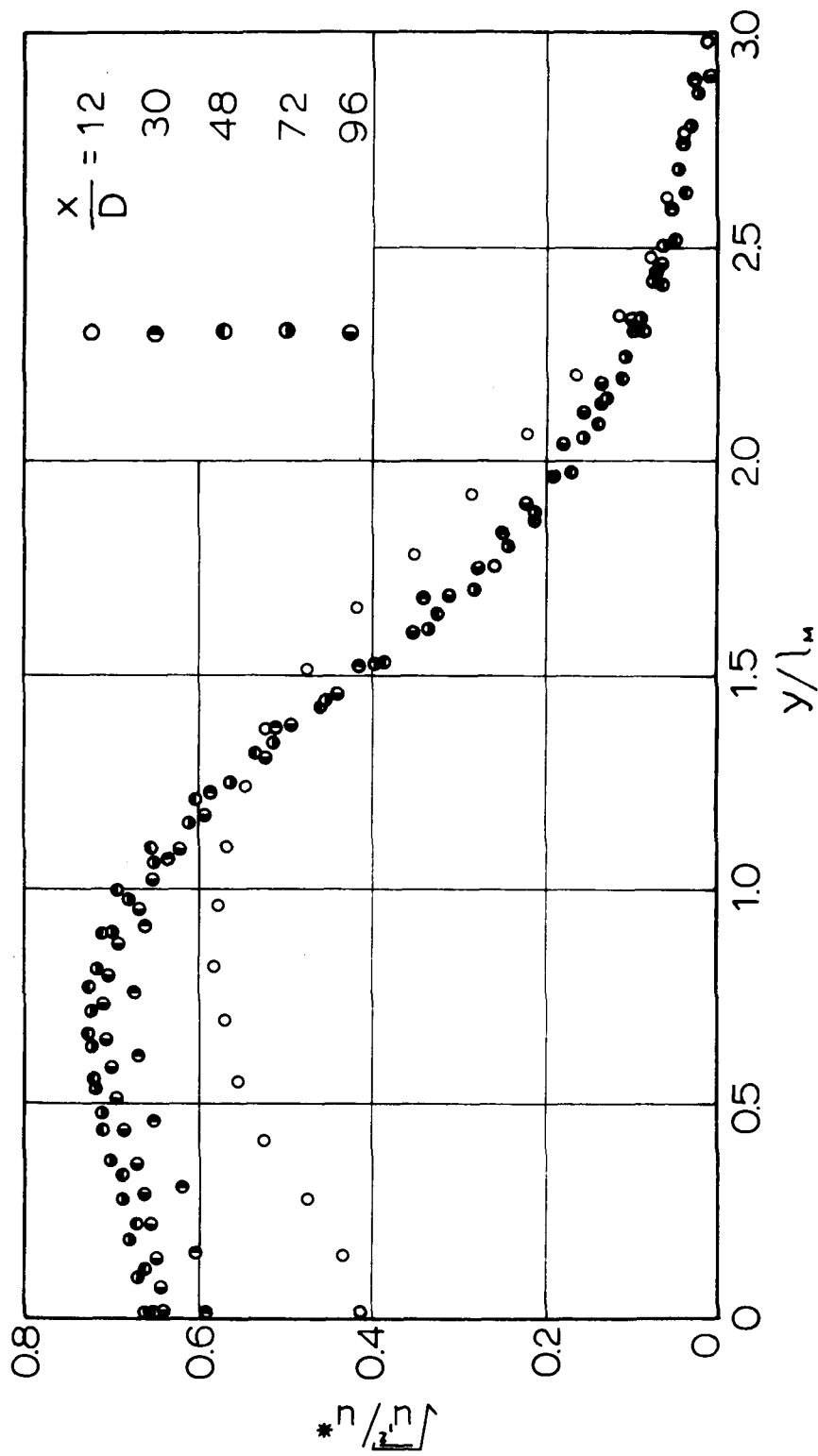


Fig. 12 Radial variation of longitudinal turbulence intensity in a round jet.  
 (Data by Ortega for  $U_j/U_0 = 2.00$ ;  $m = 0.93$ .)

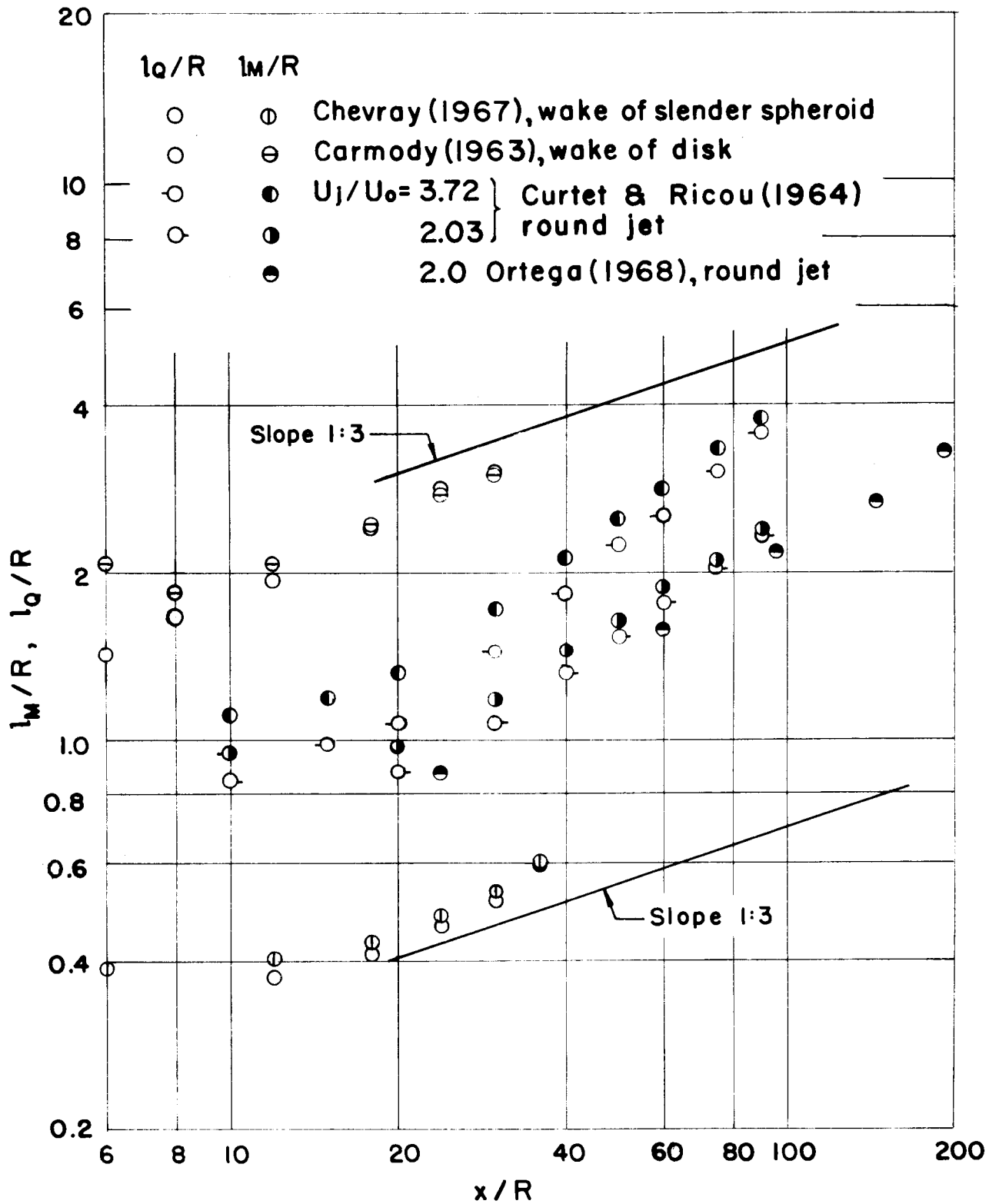


Fig. 13 Axial variation of effective width for various jet and wake flows.

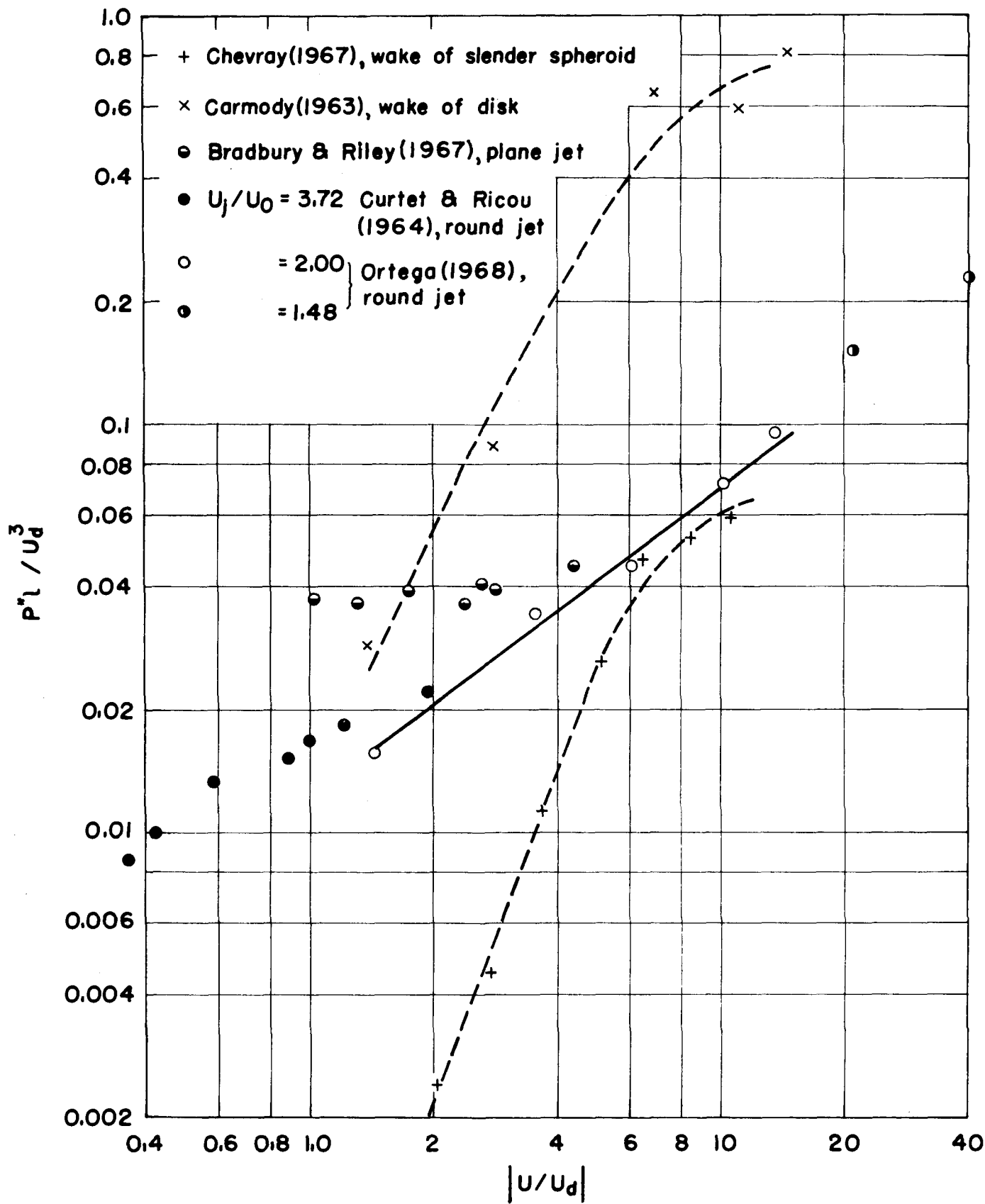


Fig. 14 Variation with  $U/U_d$  of  $P^*\ell/U_d^3$  for various jet and wake flows.

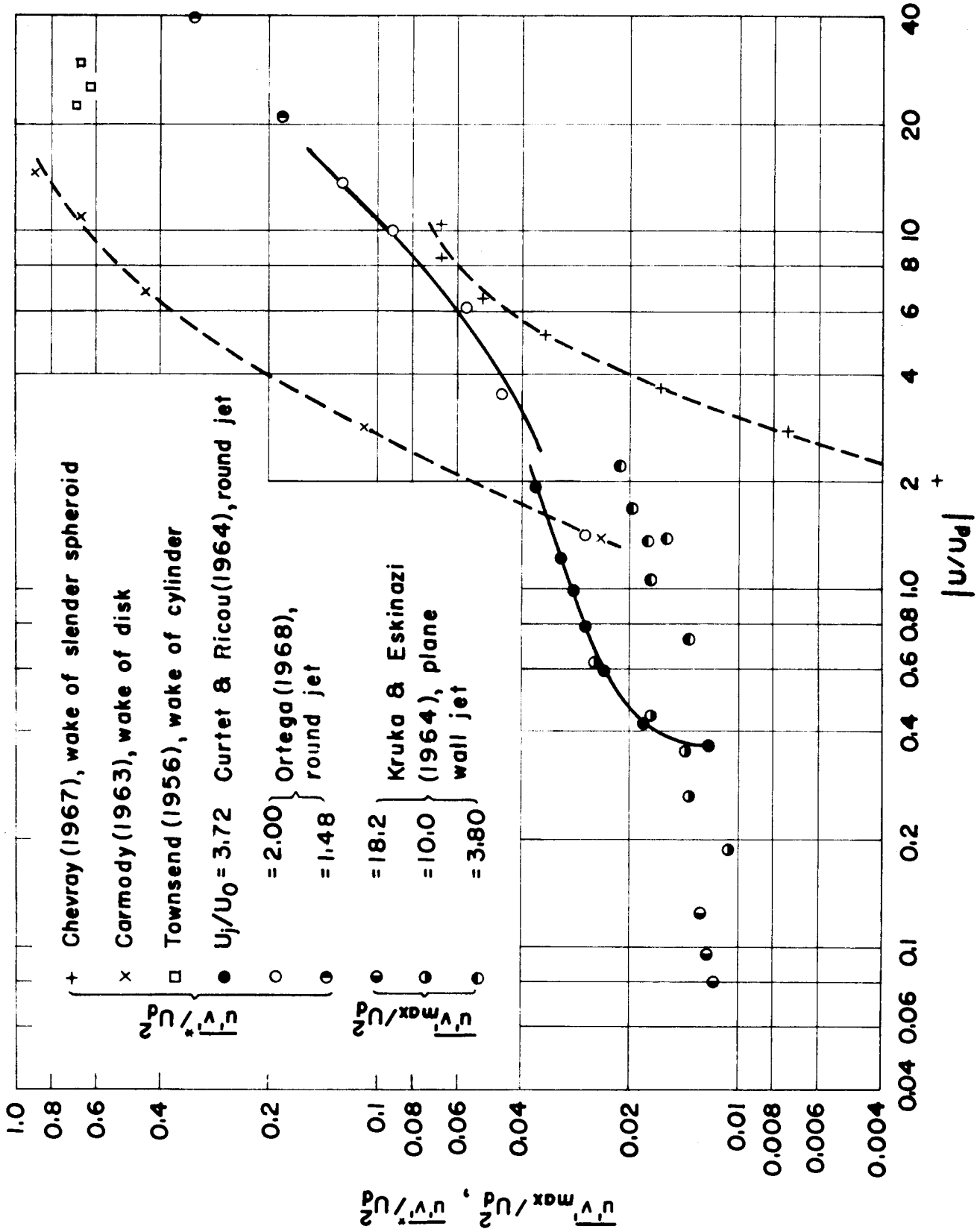


Fig. 15 Variation with  $U/U_d$  of the ratio of a characteristic cross-sectional value of  $\overline{u'v'}$  to  $U_d^2$  for various jet and wake flows.

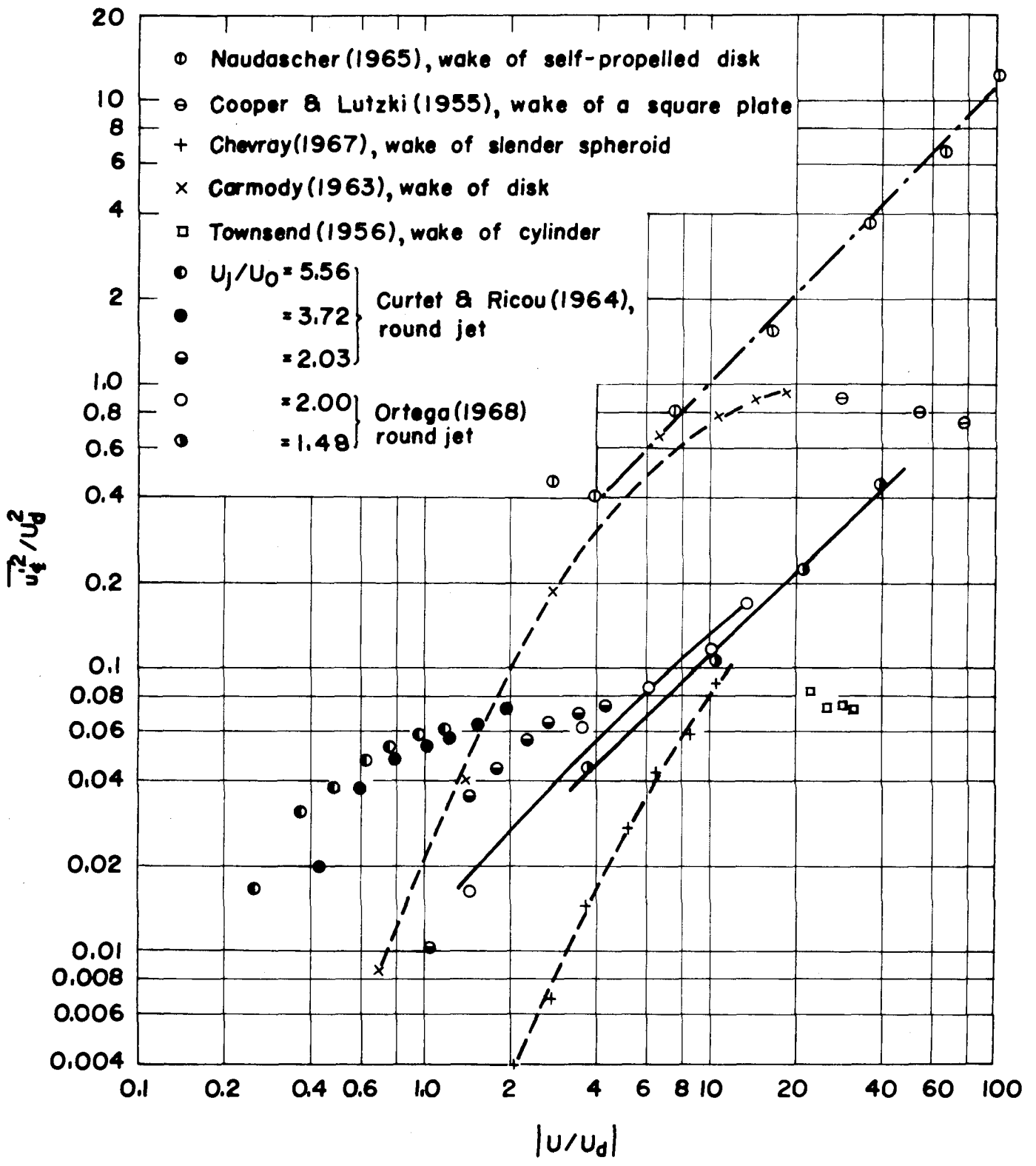


Fig. 16 Variation with  $U/U_d$  of the ratio of a characteristic cross-sectional value of  $\overline{u'^2}$  to  $U_d^2$  for various jet and wake flows.

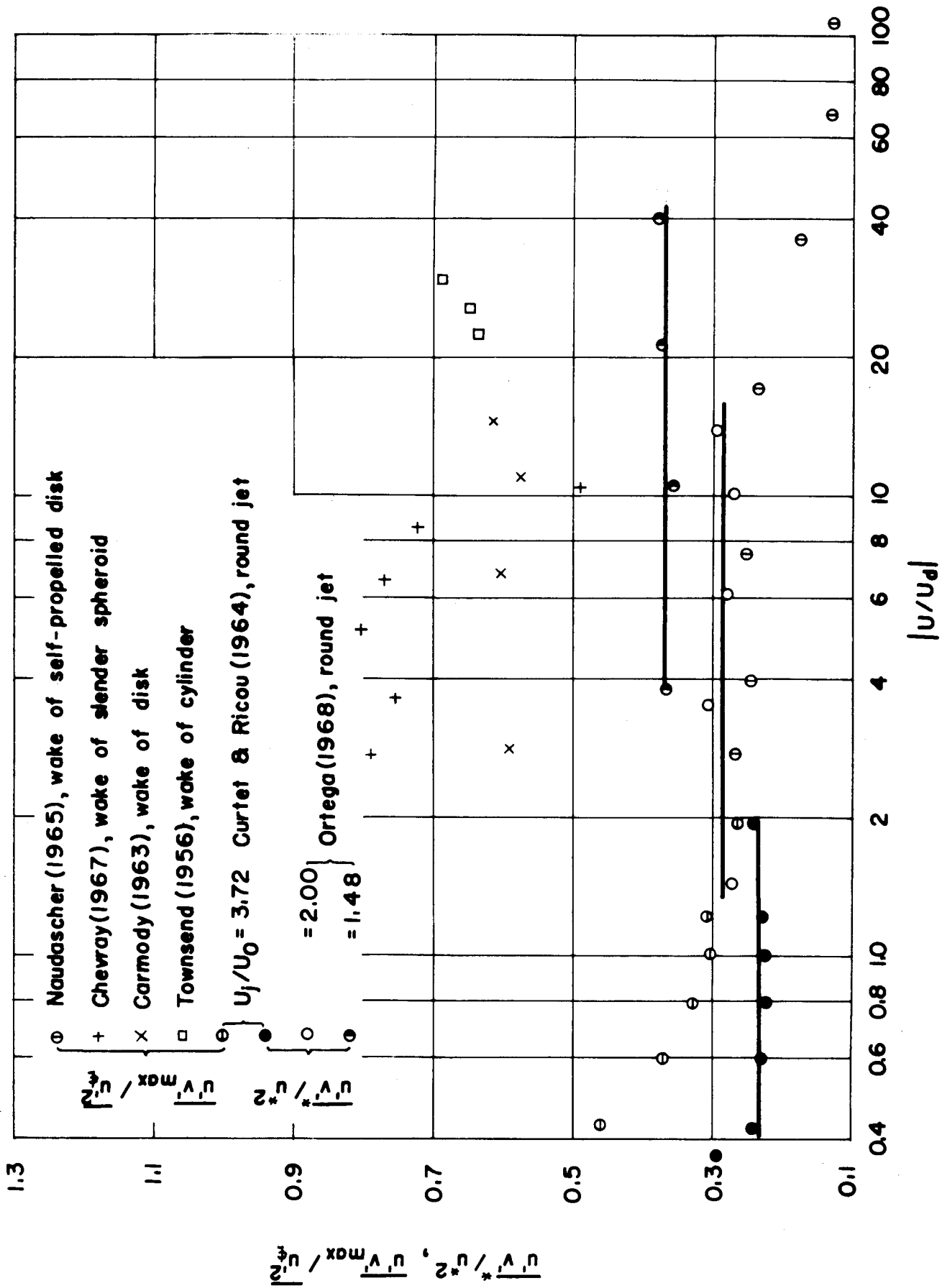


Fig. 17 Variation with  $U/U_d$  of characteristic cross-sectional values of  $u'v'/u'^2$  for various jet and wake flows.

**DOCUMENT CONTROL DATA - R & D**

*(Security classification of title, body of abstract and indexing annotation must be entered when the overall report is classified)*

1. ORIGINATING ACTIVITY (Corporate author) Iowa Institute of Hydraulic Research The University of Iowa Iowa City, Iowa 52240		2a. REPORT SECURITY CLASSIFICATION Unclassified	
		2b. GROUP	
3. REPORT TITLE  ON THE DISTRIBUTION AND DEVELOPMENT OF MEAN-FLOW AND TURBULENCE CHARACTERISTICS IN JET AND WAKE FLOWS			
4. DESCRIPTIVE NOTES (Type of report and, inclusive dates) Technical Report			
5. AUTHOR(S) (First name, middle initial, last name)  Eduard Naudascher			
6. REPORT DATE August 1968		7a. TOTAL NO. OF PAGES 37 pages	7b. NO. OF REFS 16 references
8a. CONTRACT OR GRANT NO. Nonr 1611(03)		9a. ORIGINATOR'S REPORT NUMBER(S)  IIHR Report No. 110	
b. PROJECT NO.		9b. OTHER REPORT NO(S) (Any other numbers that may be assigned this report)	
c.			
d.			
10. DISTRIBUTION STATEMENT  This document has been approved for public release and sale; its distribution is unlimited.			
11. SUPPLEMENTARY NOTES		12. SPONSORING MILITARY ACTIVITY Fluid Dynamics Branch Office of Naval Research Department of the Navy	
13. ABSTRACT  The lateral distributions of various mean-flow and turbulence characteristics, as obtained from measurements in axisymmetric jets and wakes, are shown to conform to a new concept of self-preservation. The development downstream from the flow origin of representative cross-sectional values of the turbulence shear stress $\rho u'v'$ , turbulence normal stress $\rho u'^2$ , and the maximum mean-velocity difference $U_d$ , as well as the development of some nondimensional ratios thereof, is presented for the following free-turbulence flows: plane free jets and wall jets with ambient streams, axisymmetric jets in coaxial streams with different ratios of jet to free-stream velocity, and wakes behind a slender spheroid, a disk, a square plate, and a self-propelled body of revolution. The results indicate that in the case of axisymmetric free-shear flows, similarity according to the conventional definition is not even approached asymptotically and that the conditions of flow generation have a greater influence on the downstream flow development than has been assumed previously.			

14 KEY WORDS	LINK A		LINK B		LINK C	
	ROLE	WT	ROLE	WT	ROLE	WT
(IIHR Report No. 110)  Mean Flow Turbulence Characteristics Jets Wakes						